SAND2024-16222C

Sandia National Laboratories

Developing Technologies for Composite Overwrapped Pressure Vessels (COPV) Comparing Traditional Inspections to Advanced 3-D Rendering Techniques

PRESENTED BY

John Miers, PhD.

John Miers, PhD. David G. Moore, Ciji Nelson, Caleb Schauble, Dorian K. Balch, PhD. and Elliott Jost, PhD

ENERGY NNSA

Sandia National Laboratories is a multimission laboratory managed and operated by National Technology & Engineering Solutions of Sandia, LLC, a wholly owned subsidiary of Honeywell International Inc., for the U.S. Department of Energy's National Nuclear Security Administration under contract DE-NA0003525.

Outline:

- Background and Objective
- Methods
  - Liner Inspection (Traditional Techniques)
  - Advanced Inspection UT, IR and CT
- Results
  - Pressure Experiments
  - COPV-04
  - COPV-05
  - COPV-06
  - COPV-04: Pre and Post Mortem
- Conclusions

BACKGROUND AND HISTORY

Carbon composite overwrapped pressure vessels (COPV)s have been widely used for storing gases under high pressure by NASA for space missions since the 1970s'. The principal advantage of using a solid carbon fiber reinforced plastic (CFRP) over a metallic liner is mainly for reducing weight.

Composite overwrapped pressure vessels (COPV)s are in essence pressure vessels which consist of a metal liners surrounded by a wound composite wraps.

304 Stainless Steel Threaded Float, Oblong, 3" Diameter, 6" Long

https://www.mcmaster.com

304 Stainless Steel Threaded Float, 2" Diameter, 1/4"-20 UNC Thread Size, 750 Maximum PSI

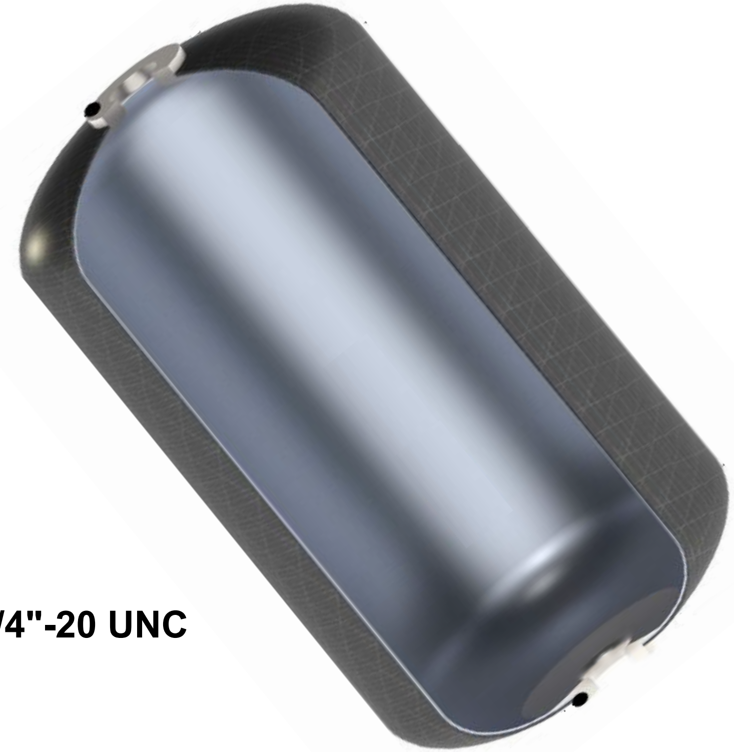

Objectives:

1. Fabricate vessels from the commercial floats and inspect with NDE
2. Prove the composite overwrap improves the strength to weight ratio

Winding Process (Steep Learning Curve)

Low cost X-winder with limited capability (no complex mandrel geometries).

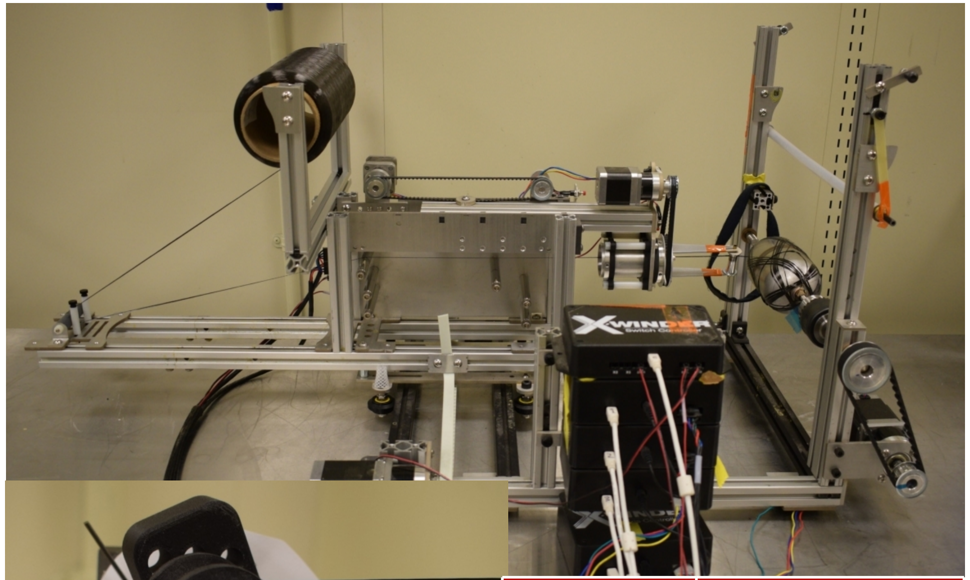

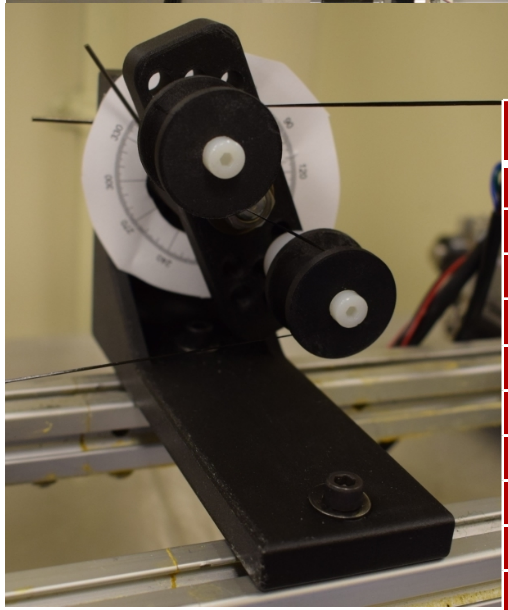

Layer	Angle (°)
1	5.8
2	65.0
3	11.5
4	75.0
5	80.0
6	20.0
7	85.0
8	90.0
9	7.0
10	90.0

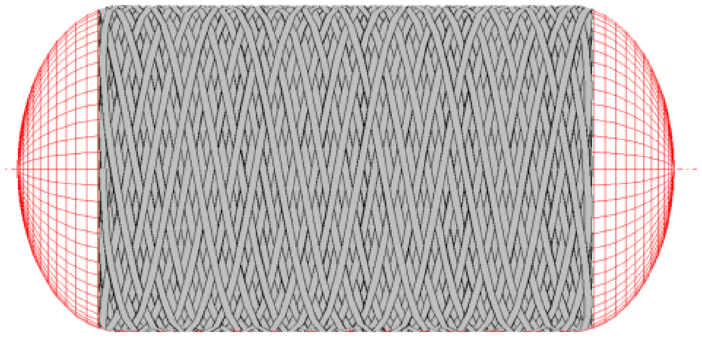

80° Layer

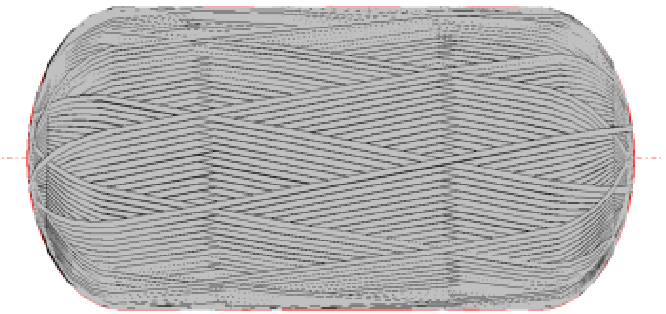

11.5° Layer

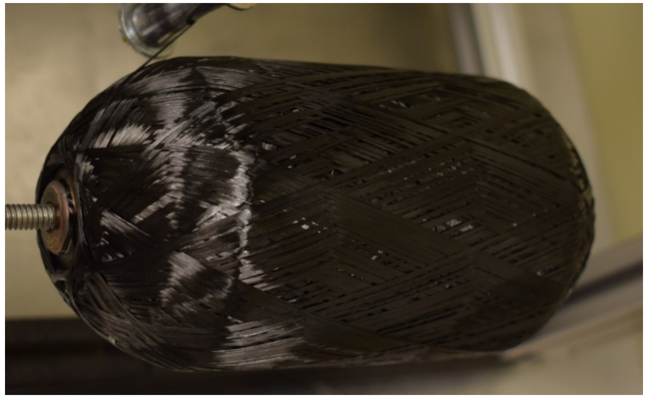

Curing Process

- Wrapped in heat shrink tape to aid with compaction
  - Developing vacuum bagging technique
- Cured in an oven with a “rotisserie” action
- Experienced some audible popping after cure
  - The composite is disbonding from liner due to residual thermal stresses (difference in linear coefficients of expansion).

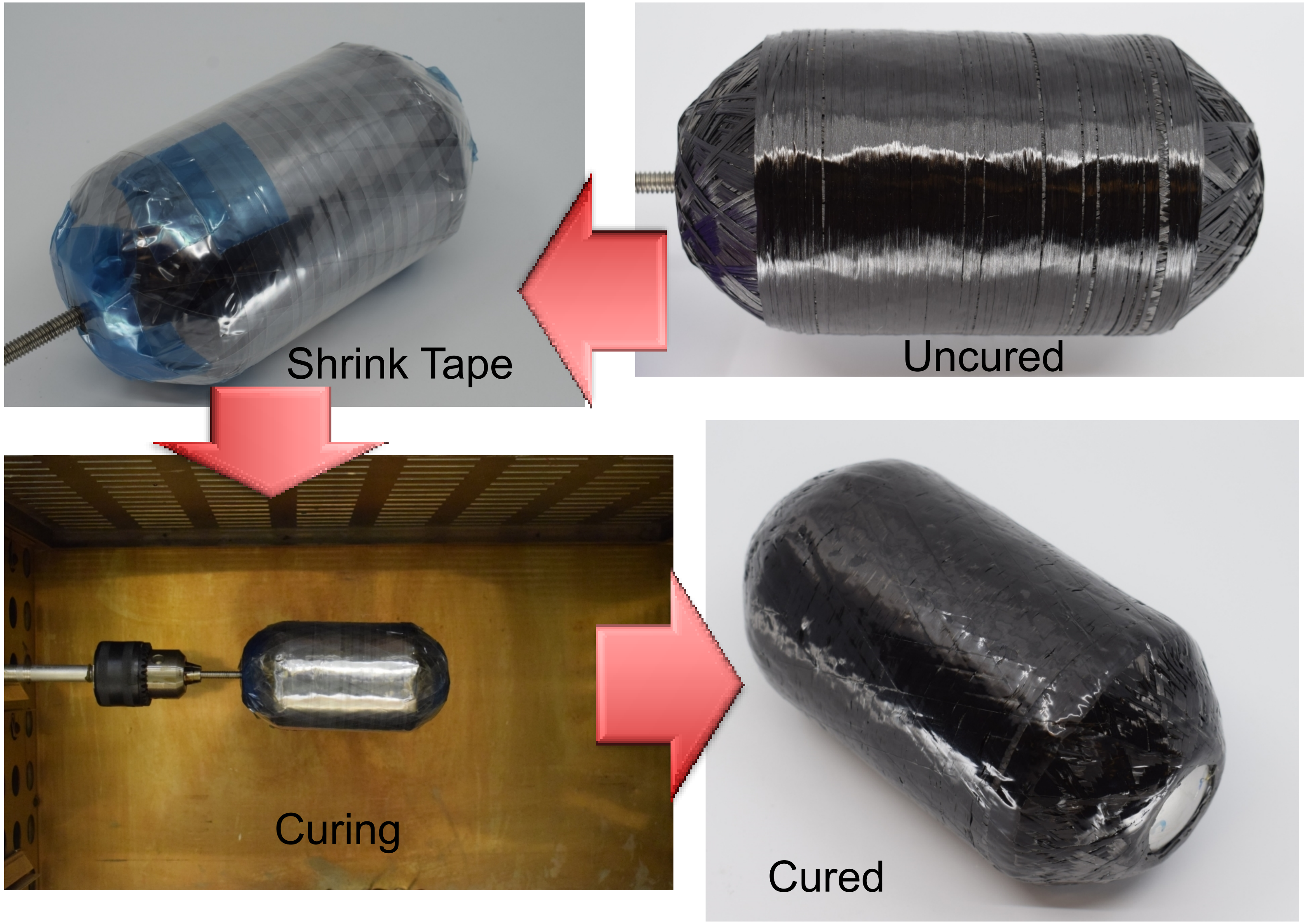

Methods: Traditional

Fluorescent Penetrant

Capabilities

- Detection of VERY small defects on the surface (≈ 5 - 10 µm)
- Crack, pore, leak detection
- Ability to inspect complex shapes

Limitations

- Defects MUST be open to the surface and the surface must be free of anything that could interfere with penetrant material
- Excess surface roughness/porosity can hide relevant defects
- Visual acuity of inspector

Eddy Current

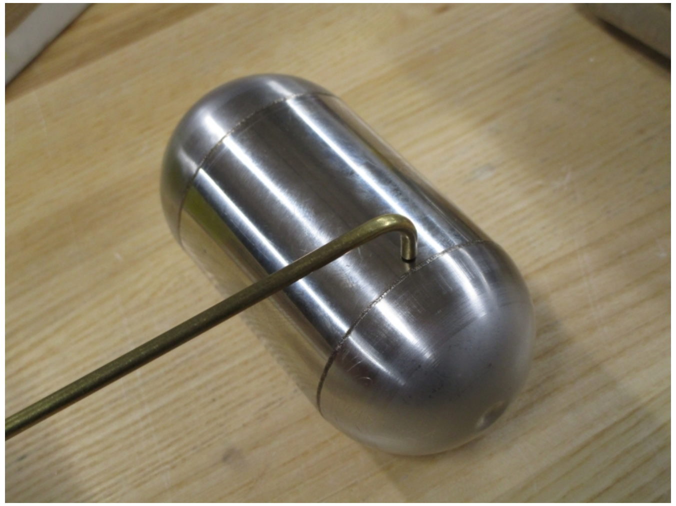

Capabilities

- Detect surface and some subsurface cracks detection.
- Metal identification and sorting using conductivity techniques.
- Measures thickness of thin metals, conductive coatings, and non-conductive coatings on conductive substrate.

Disadvantages

- Hand-held systems are generally used in localized small areas but can be automated on surfaces.
- The surface of the inspection area must be clean.
- Several human factors: probe lift off and physical positioning can impact results. Effective inspection depth in a material is ¼" up to ½" max.

Methods: Ultrasonic and Thermography

UT

- UT waves
  - Wave speed: speed of the wave's propagation
  - Acoustic impedance: material's resistance to the propagation
  - Impedance ratio: how much energy is reflected back due to interference at material boundaries

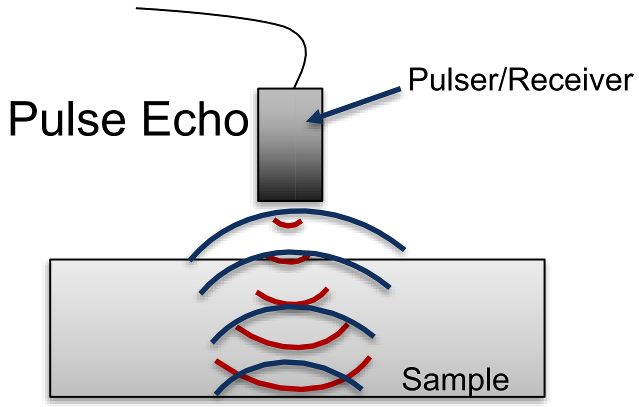

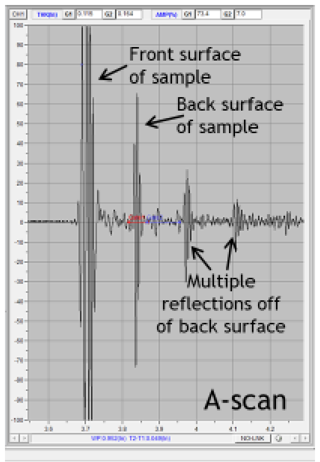

IR

- Thermographs from thermal camera
  - Images show thermal radiation
  - Active thermography: stimulus to heat surface and observe the surface characteristics with infrared camera

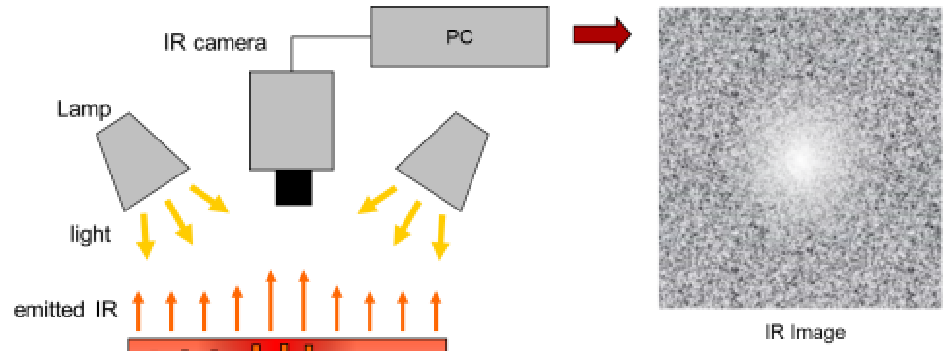

Source: Thermal Wave Imaging

Methods: Computed Tomography

- Computed tomography (CT):
  - Measures attenuation of the x-ray through a material over an angular sweep of projections.
  - Data is collected in radiographs and reconstructed to produce a 3D model of the part both internal and external.
  - Volumetric data set is produced

Sample	Carbon Wrap Over Stainless Steel Liner		
Energy	200 kV	Projections	3000
Current	255 µA	Effective Pixel Size	~ 56 µm
Magnification	2.26X	Detector Type	Varian L08
Filter	0.52mm Cu, 0.4mmAl	X-ray Head Type	XRayWorX
Time	72 minutes	Frame Average	*6 Frame average per projection*

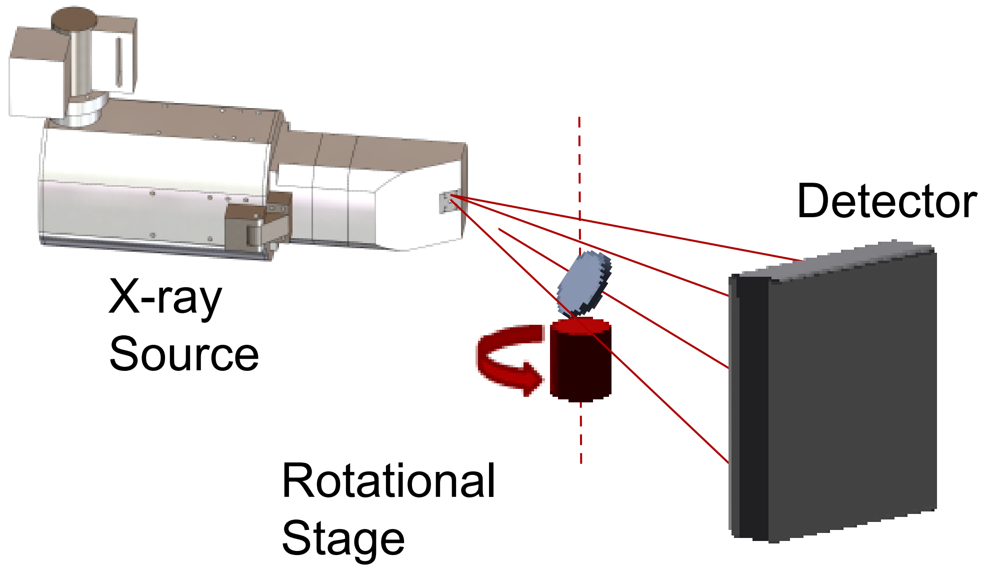

Pressure Experiments

Liner 1 (real time and high speed video)

SN	Float Type	Burst Pressure psi	Time elapsed	Location of failure
01	Liner	3873psi	12: 05 min	Waist weld
02	Liner	3733psi	8:55 min	Waist weld
03	Liner	3601psi	6:54 min	Waist weld
04	Overwrap marked “1”	7413psi	10:00 min	Waist weld
05	Overwrap w/adhesive marked “3”	5250psi	~5 min	Waist weld (bleed out to top curve)
06	Overwrap marked “2”/Flawed	No burst; leaked around 7ksi	~10 min	Nozzle weld

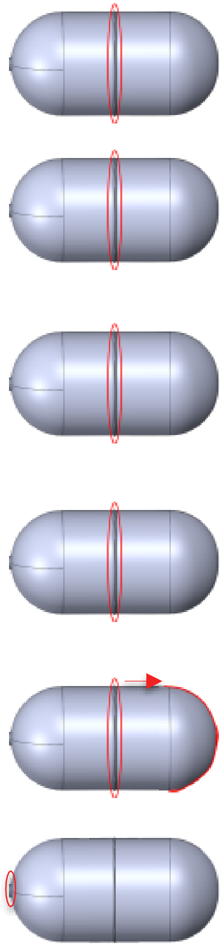

Edgertronic Camera: frame rate was 10k frames per second with a camera resolution of 1280 by 1280.

Results: Penetrant, Eddy Current, and UT

- Samples 01 and 02 showed signs of defects at the weld lines as shown bellow

Part No.	Indications	Notes
I	Yes, pit	A pit was detected on the weld surface during the penetrant inspection.
II	Yes, lap	Small lap was detected during the penetrant inspection.

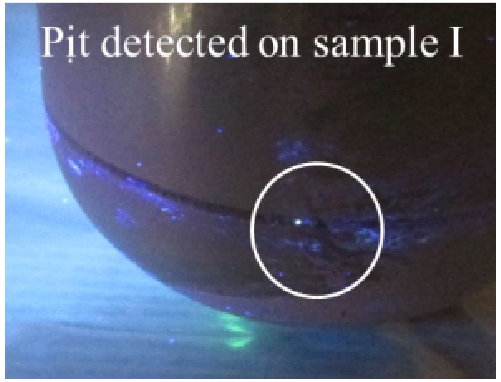

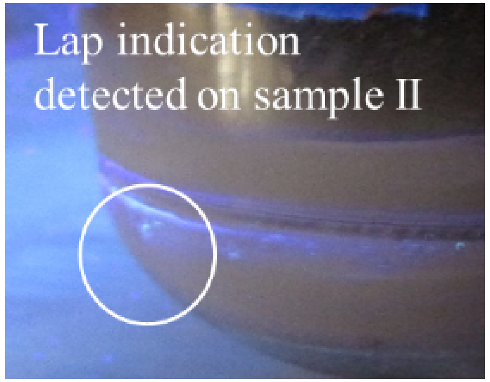

- No indications were detected with Eddy current

- Ultrasonic C-scan images reveal the weave pattern of sample 04 (barrel section only)

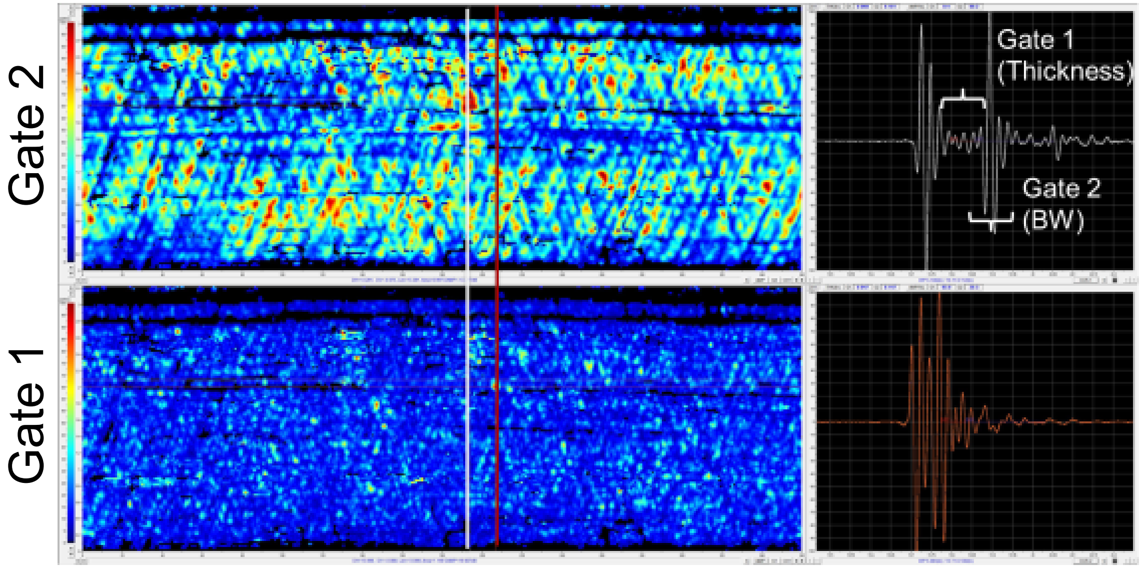

- Top image shows the backwall signal amplitude – (interface of the composite and metal liner)
- Bottom image shows amplitude between surface and backwall of composite (composite thickness)

COPV-04: UT and IR

- Thermography
  - All images taken 12.9 seconds after flash

Time slice of reconstructed raw

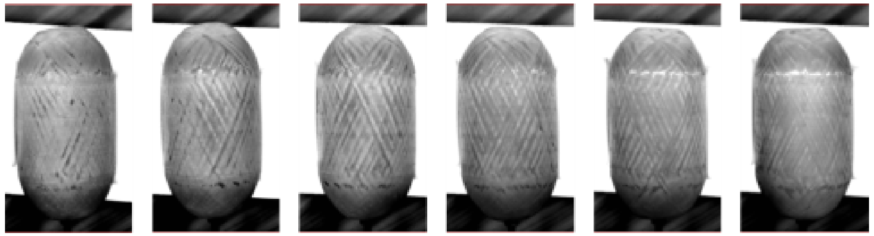

Time slice of reconstructed (first derivate)

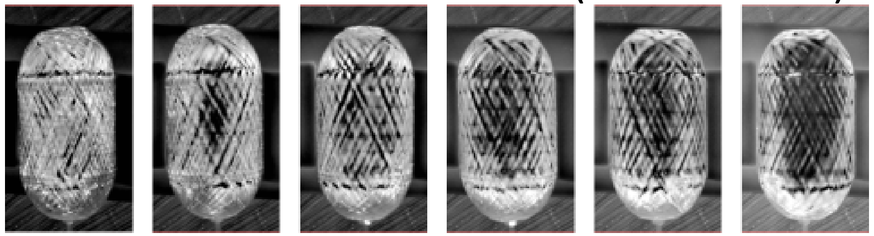

Time slice of reconstructed (second derivate)

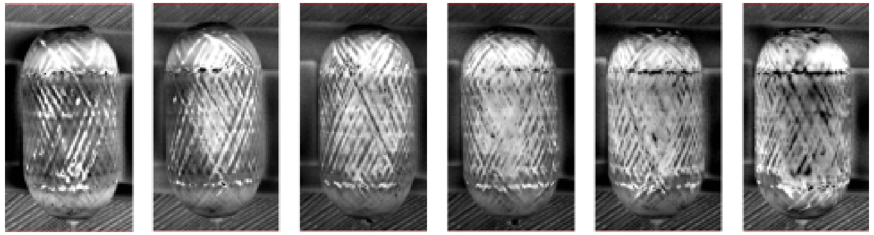

- UT vs IR

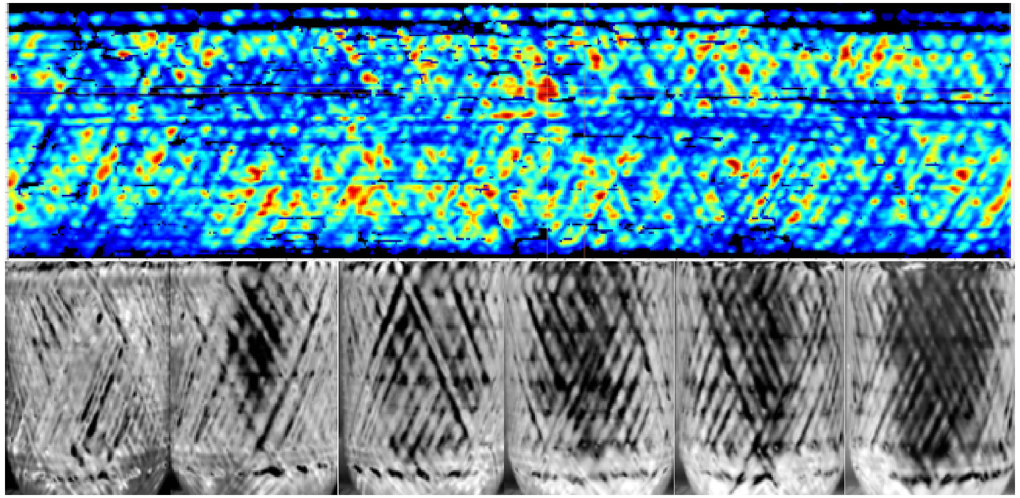

  - Bonded area transmits sound into the liner (blue)
  - Poorly bonded area reflects sound to the probe (red)
  - Correlation between UT and thermographic results

Computed Tomography

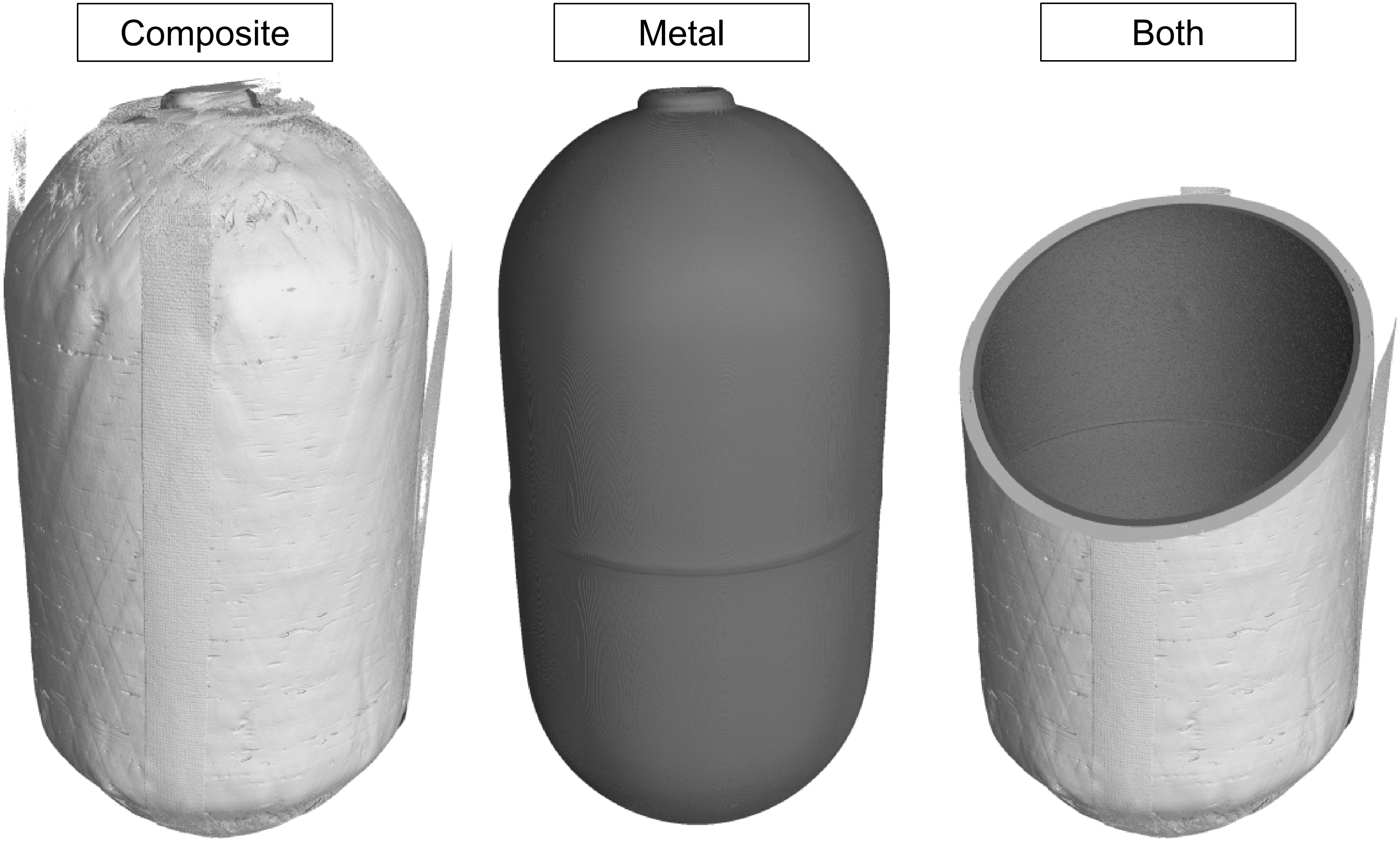

COPV-04

- Liner
  - No major defects
  - Minor splatter in waist weld
  - Minor misalignment in regions of waist weld
- Composite
  - Porosity/voids
  - Well bonded to liner
  - Quality decreases at transition from cylindrical to spherical surfaces of the liner

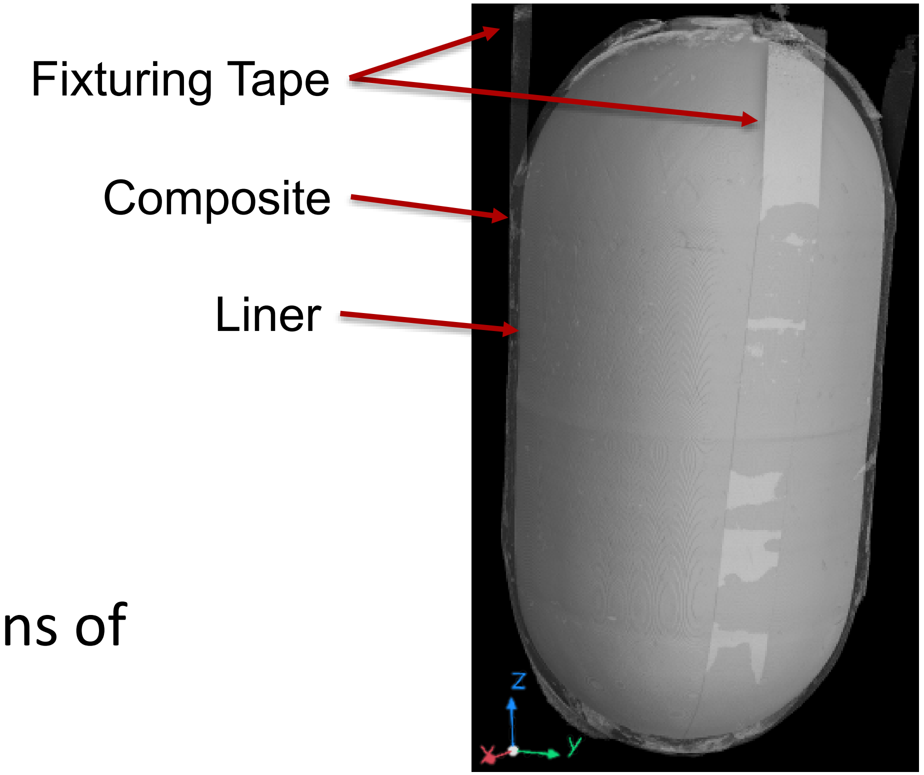

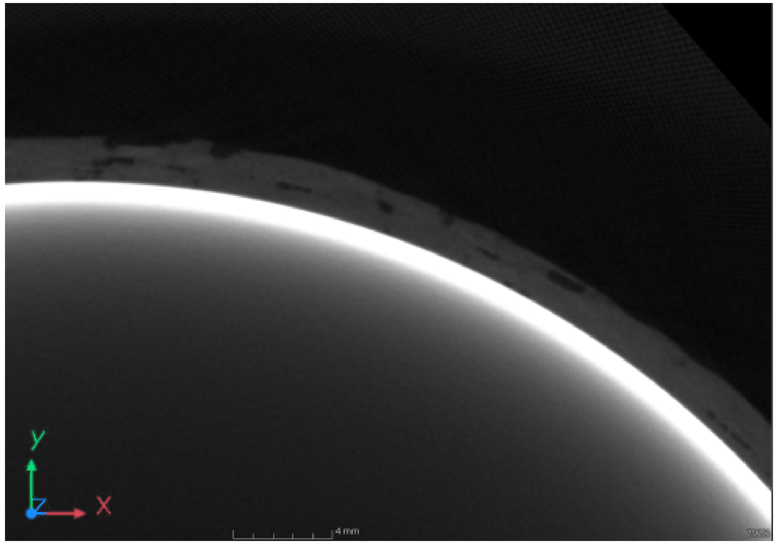

COPV-05

- Low pressure failure is due to break/gap in the waist weld
- Propagation of pressurized fluid along the poor bond between the liner and composite

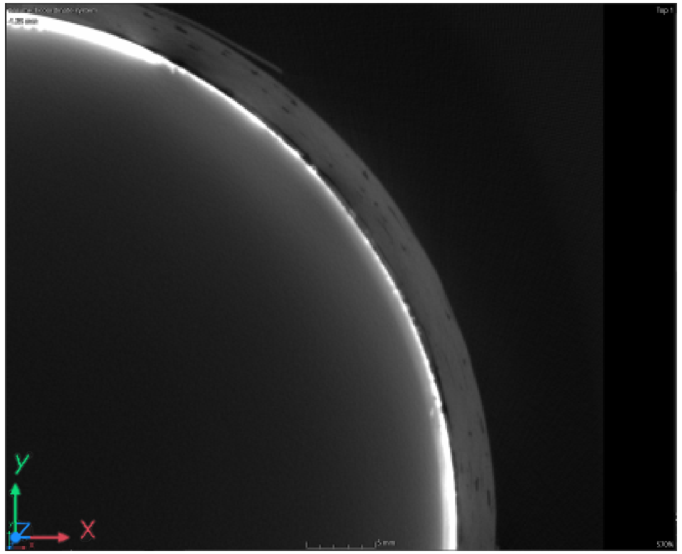

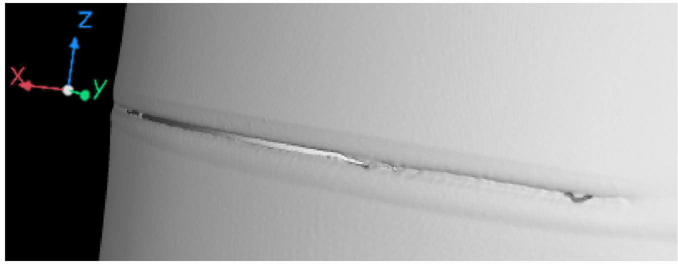

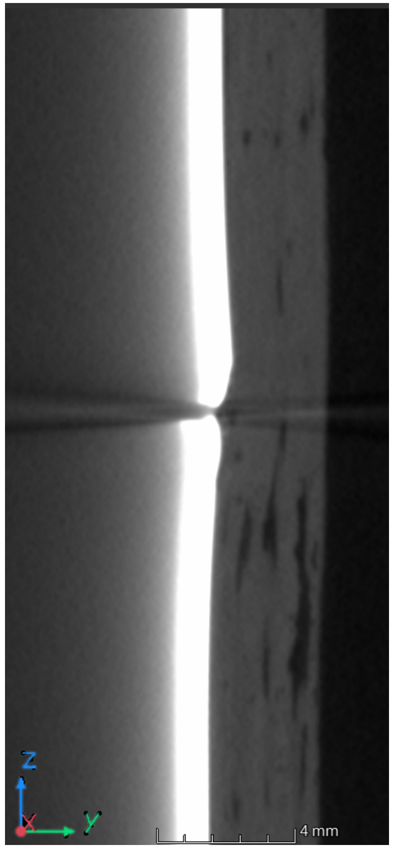

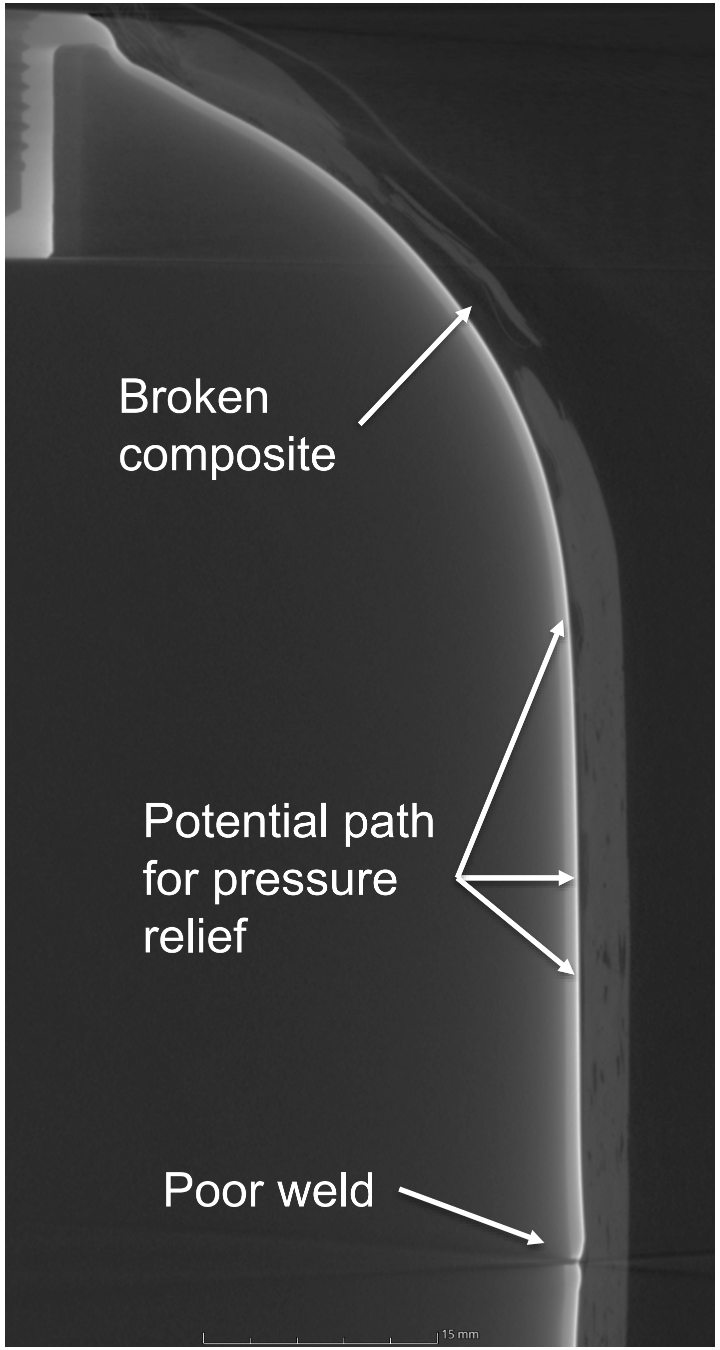

COPV-05

- Inspection of composite quality

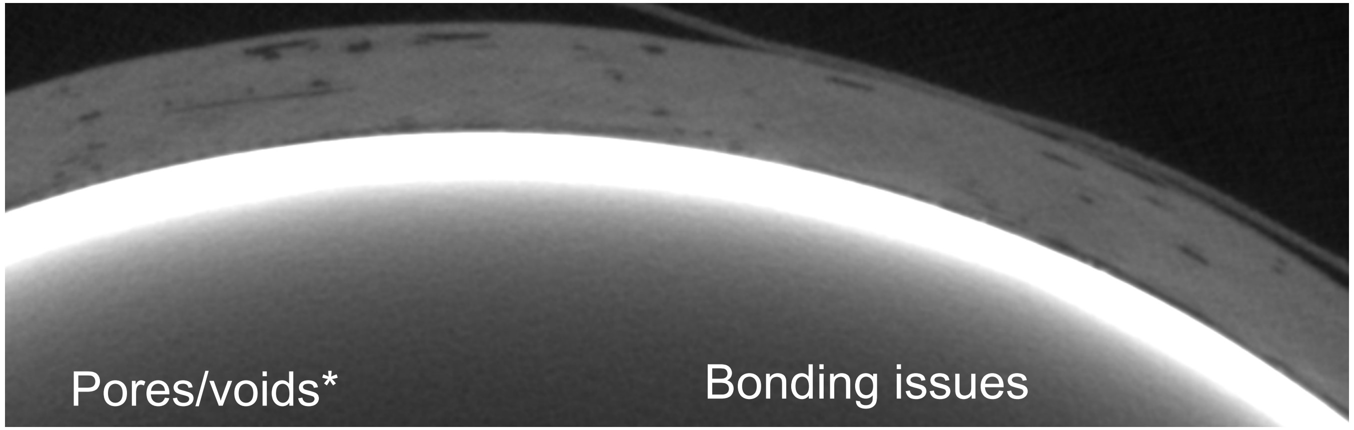

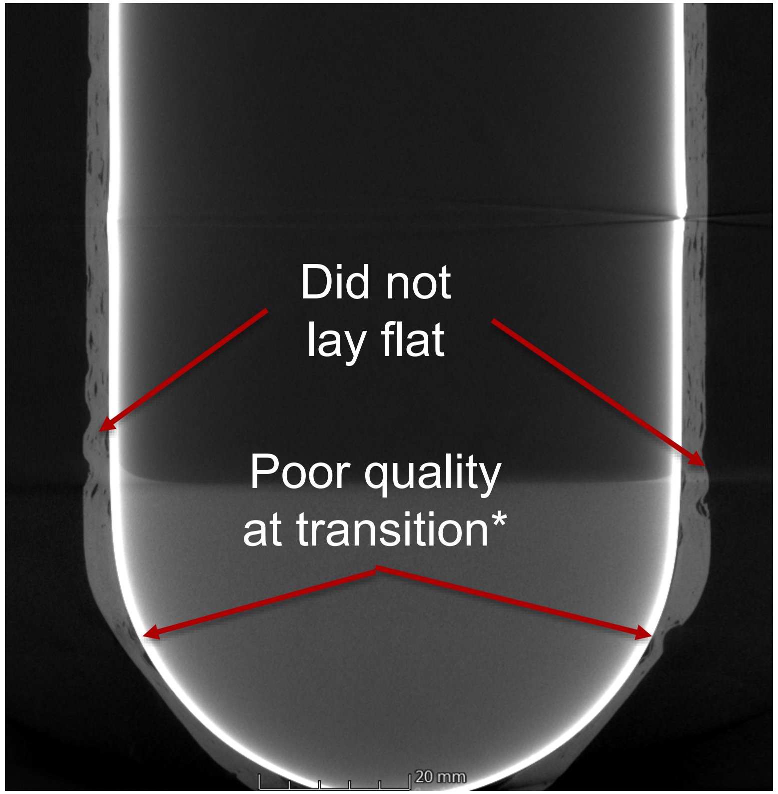

Composite Fly-Thru

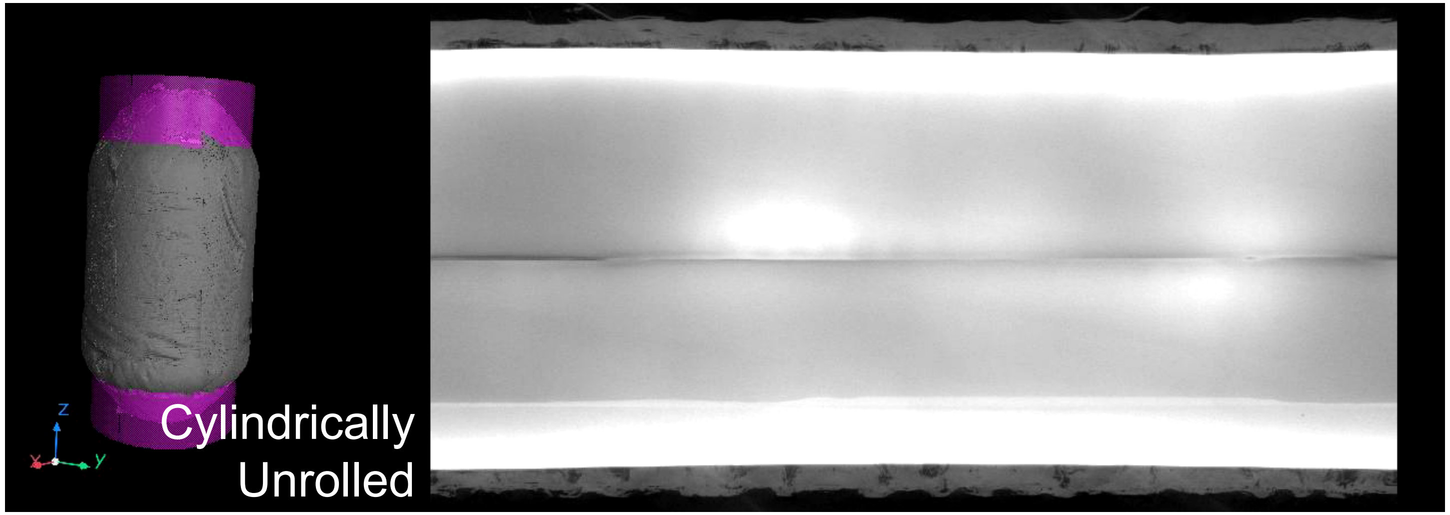

*True for all samples shown in presentation

COPV-06

- Introduced intentional defects in metal liner
  - Linear defects with utility knife, file, and hacksaw
  - Point defects with hammer and punch
  - Determine if NDE can detect

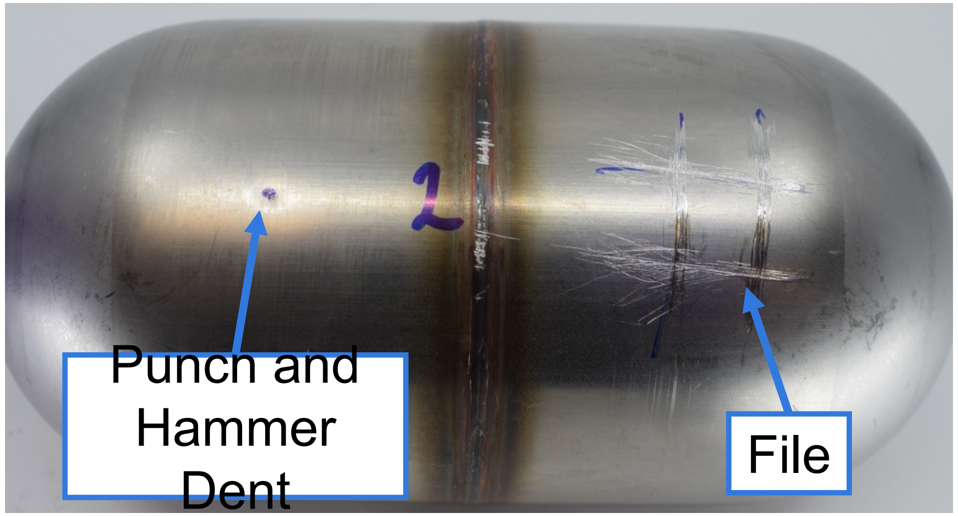

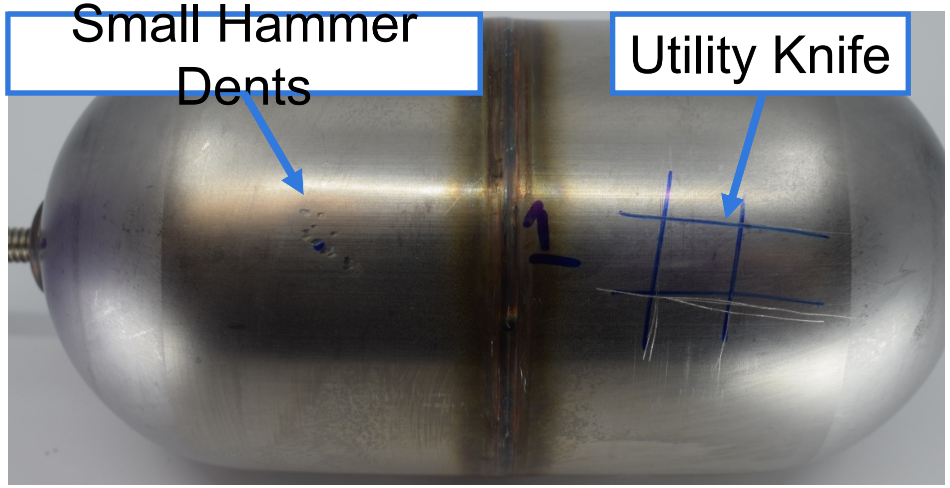

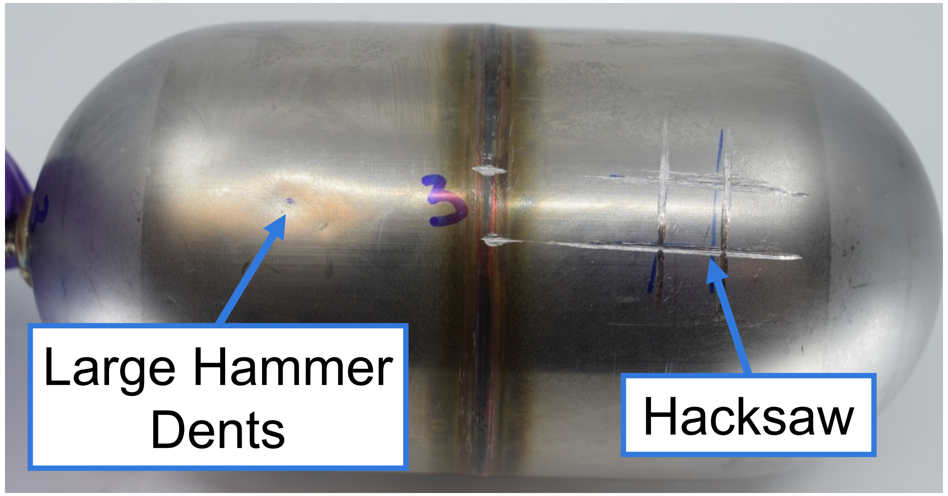

COPV-06: Detection of Intentional Defects

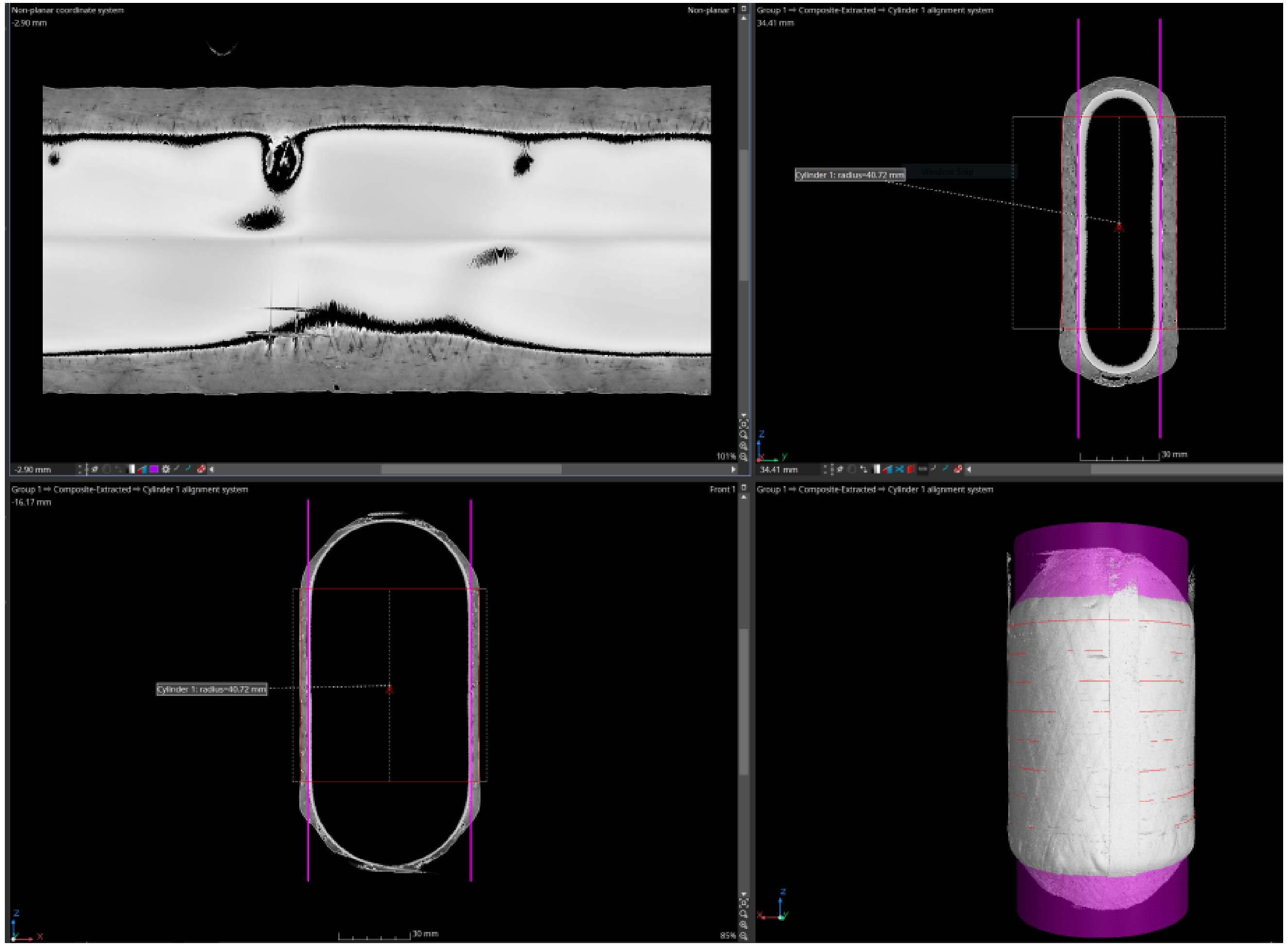

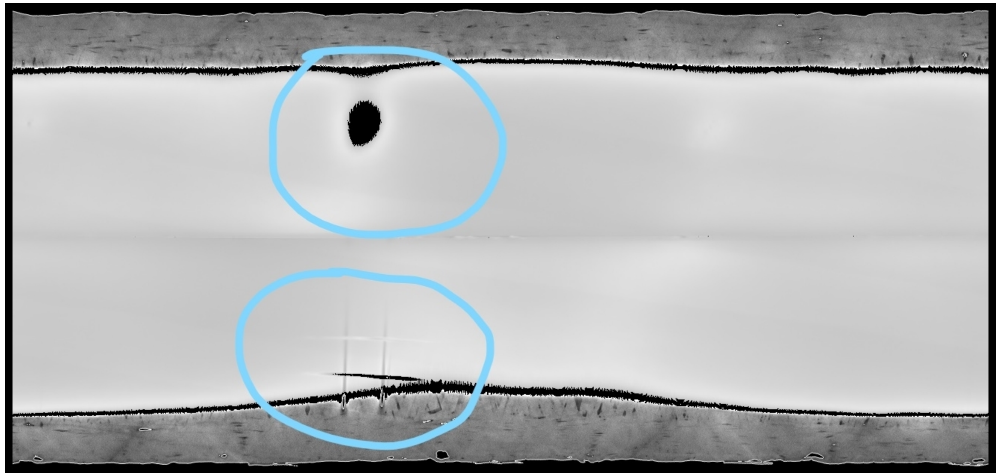

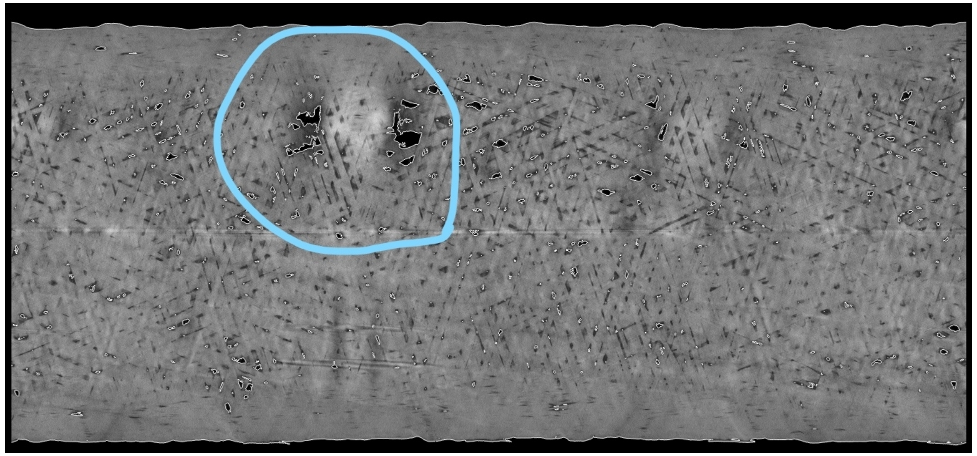

COPV-06

- Detection of non-intentional defects
  - Waist weld quality
  - Cracking in nozzle weld
    - Culprit for leaking in burst test

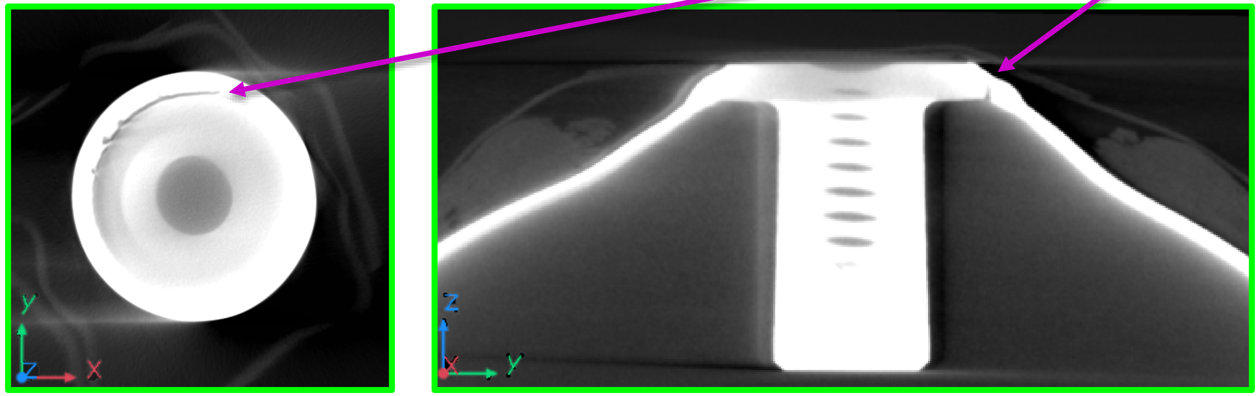

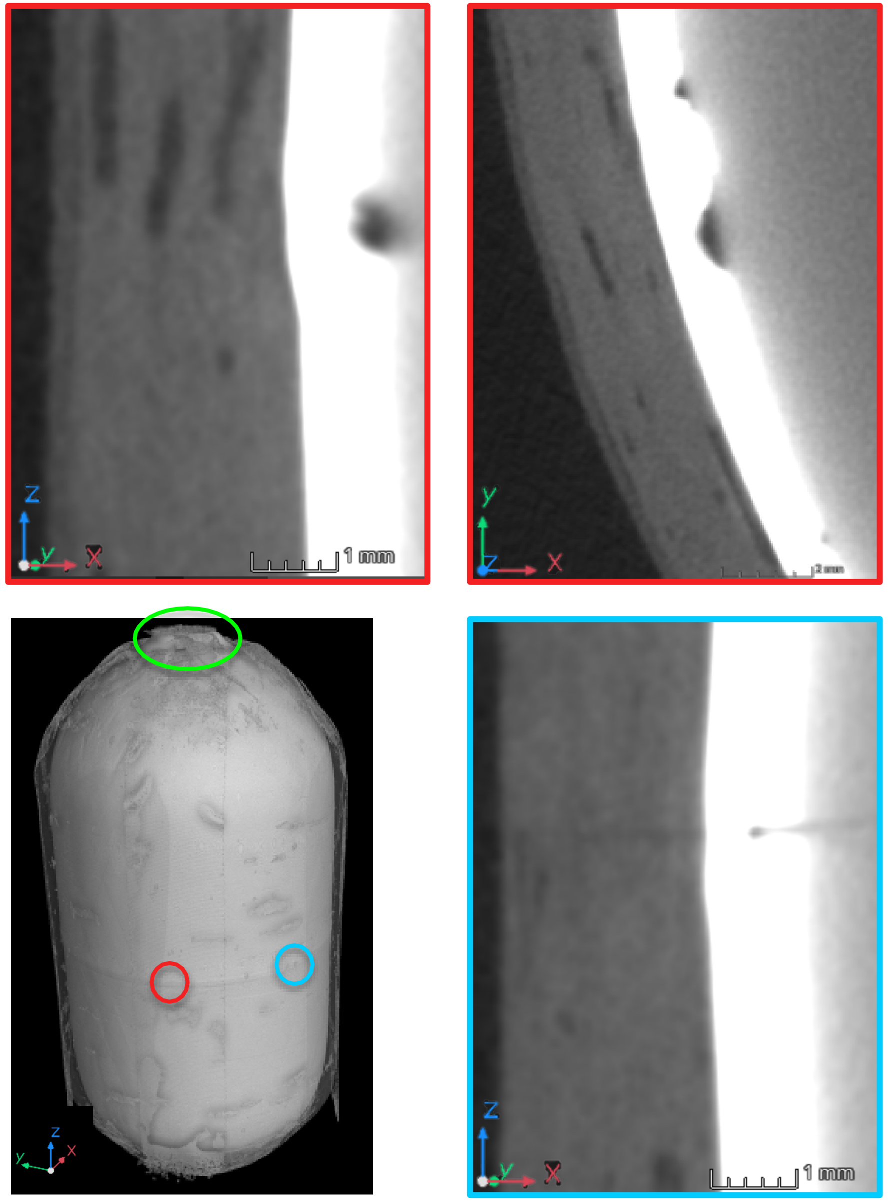

COPV-04: Pre and Post Mortem

COPV 4 (real time)

COPV 4 (high speed video)

Edgertronic Camera: frame rate was 10k frames per second with a camera resolution of 1280 by 1280.

COPV-04: Pre and Post Mortem

- Pre-test weld line
  - Rotation fly-thru

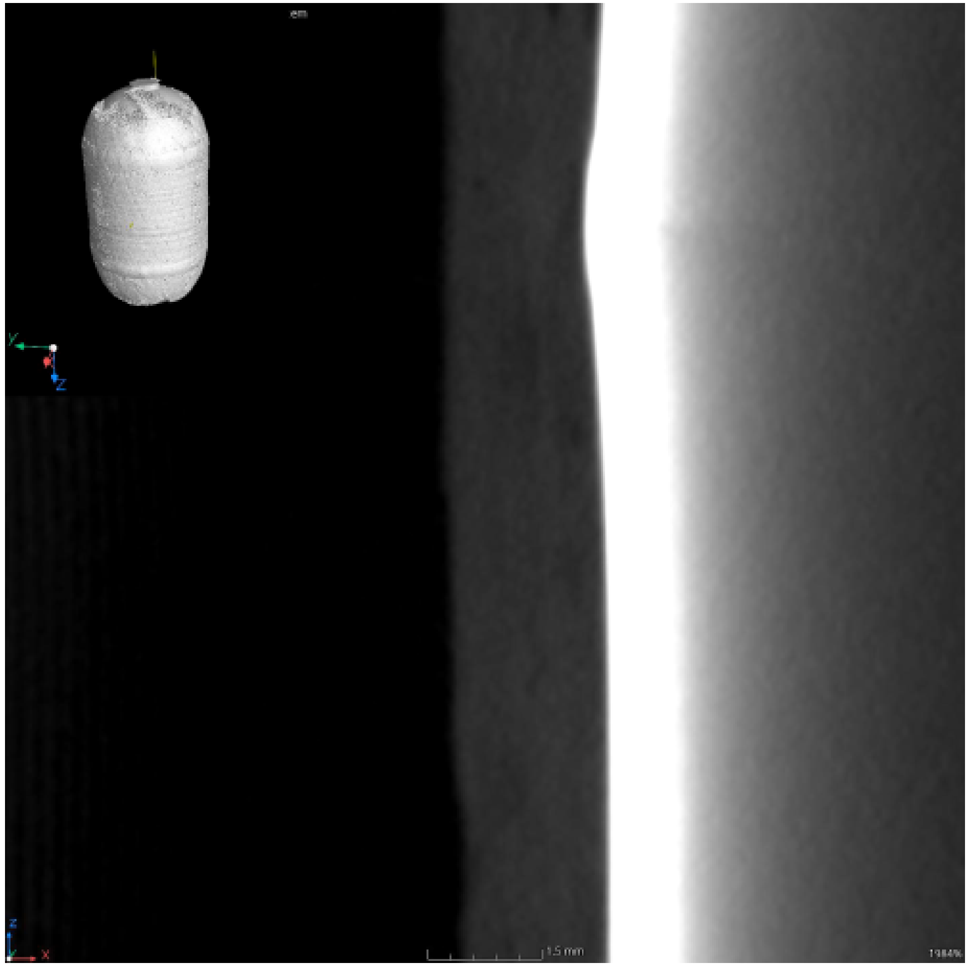

- Post-test weld line
  - Rotation fly-thru

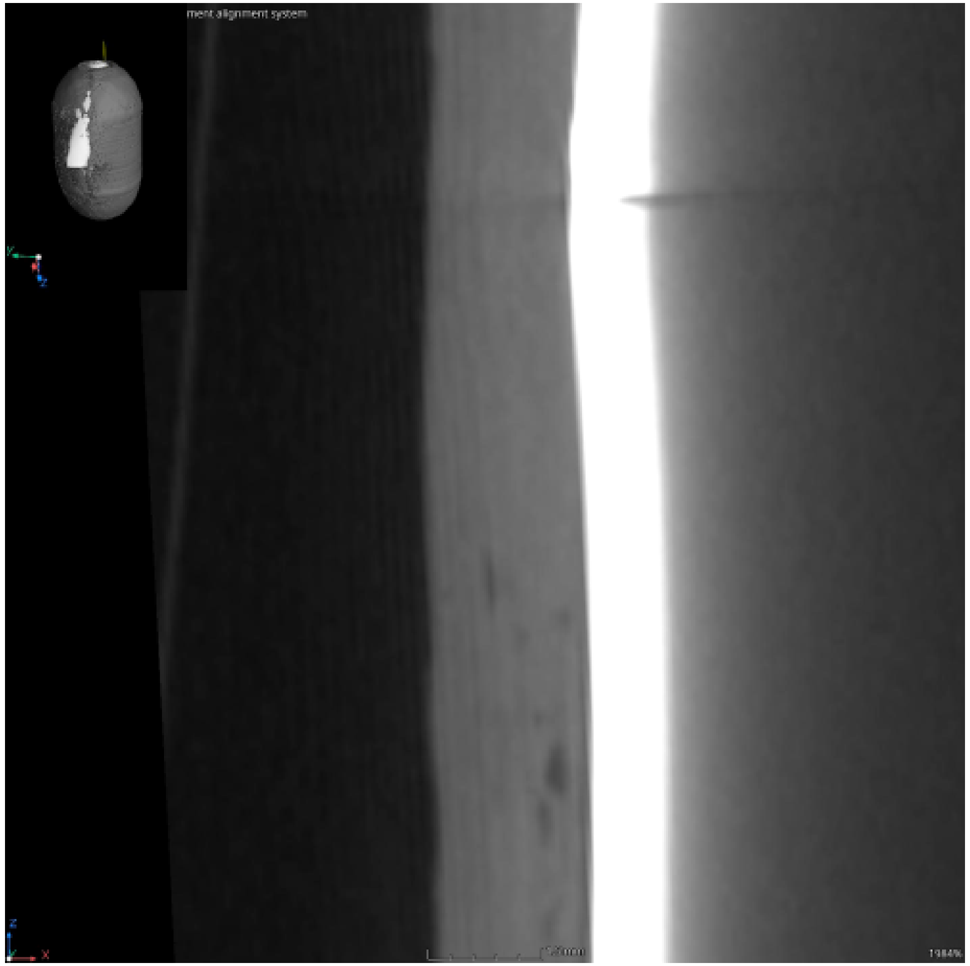

COPV-04: Pre and Post Mortem

- Initial waist weld quality was among the best inspected
- Only minor defects and porosity in the composite overwrap
- Consequently the sample performed the best in the burst test
  - Yielded a 22 kJ/kg increase in pressure vessel efficiency over solo liners tested
- Waist weld failed at liner offset and region of minimal weld depth
- Ductile deformation in weld due to pressurization (thinning)
  - Ductile thinning → weld failure
  - Potential for modelling

Conclusions

- The ultrasonic elastic wave interacts with the composite fiber structure.
- Ability for UT to detect the bondline variance are:
  - Composite surface texture
  - Fiber orientation
  - Binder concentration
- Signal loss due to sound dispersion and absorption making the bondline interface hard to detect
- Shiny surfaces hinder the infrared technique and cause large “noise” signals
  - Low reflectivity paint might alleviate
- A CT inspection technique was developed which segments the multi-material data into composite and metal regions
  - Wrapping patterns are difficult to estimate
  - Single layer fibers are not distinguishable
  - The damaged liner was easy to detect
  - Debonding can be detected
  - Weld issues can be detected

Conclusions

- Weld quality varied across the samples, but pores, liner misalignment, and occasional weld spatter/roughness were common
- Failure typically occurs due to issues in the waist weld of the liners
  - Commercially purchased
  - Better quality is obtainable
- Composite bonding plays a significant role in COPV strength
  - Poor bonding between composite and liner allows for the liner to expand and early weld failure to occur
  - Ability of the pressurized material to seek out weak points in the composite is a function of the quality of the composite to liner bondline interface

BURST TESTING RESULTS

Float SN	Weight (g)	Diameter (inches)	
Liner 01	254.64	120°	2.99
		240°	3.01
		360°	2.97
Liner 02	249.52	120°	2.99
		240°	2.99
		360°	3.00
Liner 03	249.94	120°	2.98
		240°	3.00
		360°	3.00
COPV 04	365.80	120°	3.14
		240°	3.14
		360°	3.14
COPV 05 Adhesive	416.76	120°	3.25
		240°	3.24
		360°	3.23
COPV 06	398.64	120°	3.22
		240°	3.21
		360°	3.21

SN	Float Type	Burst Pressure psi	Time elapsed	Location of failure
01	Liner	3873psi	12: 05 min	Waist weld
02	Liner	3733psi	8:55 min	Waist weld
03	Liner	3601psi	6:54 min	Waist weld
04	Overwrap marked “1”	7413psi	10:00 min	Waist weld
05	Overwrap w/adhesive marked “3”	5250psi	~5 min	Top Curve
06	Overwrap marked “2”/Flawed	No burst; leaked around 7ksi	~10 min	Inside

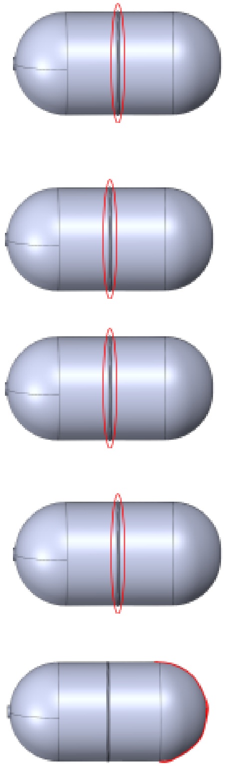

Wave Scatter Theory

Materials that demonstrate frequency dependent velocity variation are known as dispersive materials. In these types of materials there is a distinction made between the group velocity and the phase velocity.

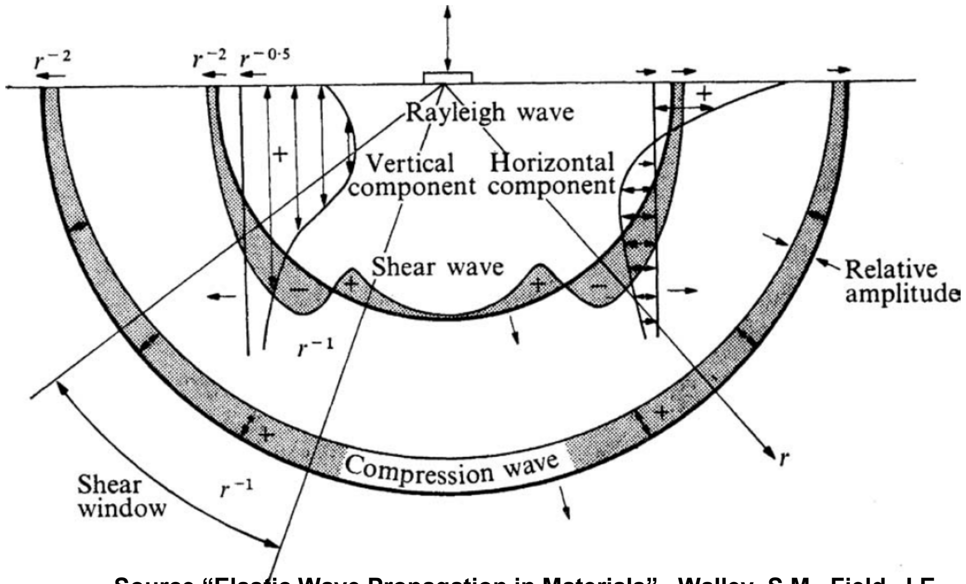

Source “Elastic Wave Propagation in Materials” , Walley, S.M., Field, J.E. Materials Science and Technology, Elsevier 2005.

$$v_g = v_p + f\frac{\delta v_p}{\delta f}$$

Group velocity (v_g) is defined as a rate at which the point of maximum amplitude in the ultrasonic pulse (many frequencies) propagates through the material.

Phase velocity (v_p) is defined as the velocity of a continuous sinusoidal wave (one frequency) in the material.

These two velocities are related to each other through dispersive properties (frequency dependence of the phase velocity).

Plane Wave in Orthotropic Materials

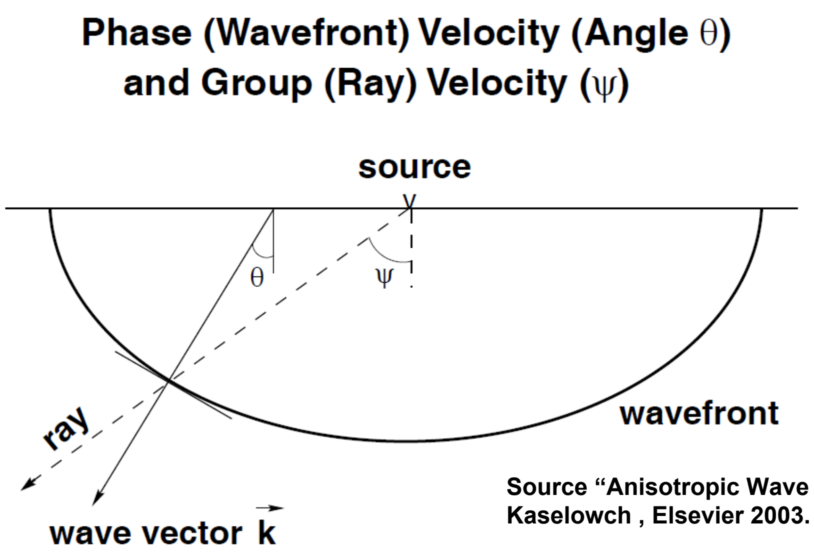

Source “Anisotropic Wave Propagation”, Kaselowch , Elsevier 2003.

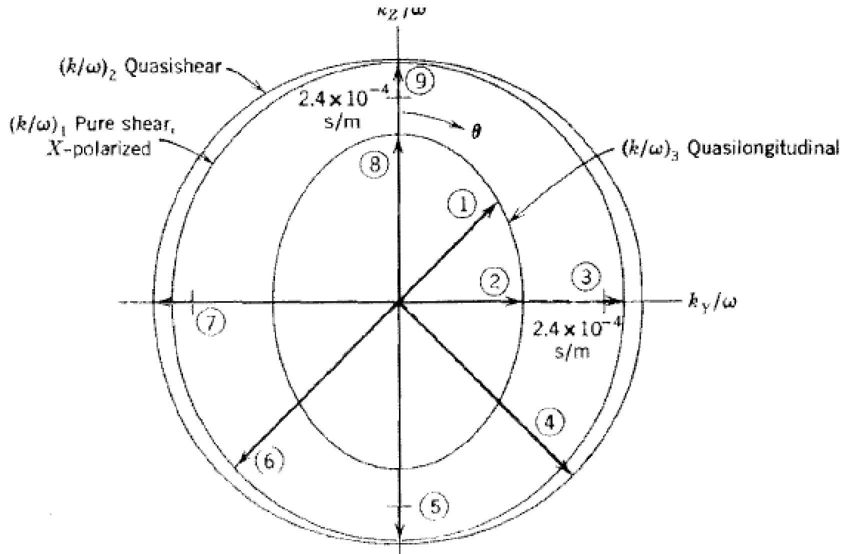

Source “Acoustic Fields and Waves in Solids”, Appendix 3 , B. A. Bauld, Wiley, New York 1973.

The elastic modulus for composite materials is generally not isotropic in nature, but is orthotropic. Most composites contain voids and micro-cracks within the structure. These manufacturing anomalies result in; a higher ultrasonic noise and texture appearance in the inspection images.

Sound dispersion and absorption causes signal losses as thickness increases. All these variables make the bondline interface between metals and composites more difficult to detect and quantify.

Orthotropic Materials Properties

$$
\begin{bmatrix} \varepsilon_{xx} \\ \varepsilon_{yy} \\ \varepsilon_{zz} \\ \varepsilon_{yz} \\ \varepsilon_{zx} \\ \varepsilon_{xy} \end{bmatrix} = \begin{bmatrix} \frac{1}{E_x} & -\frac{v_{yx}}{E_y} & -\frac{v_{zx}}{E_z} & 0 & 0 & 0 \\ -\frac{v_{xy}}{E_x} & \frac{1}{E_y} & -\frac{v_{zy}}{E_z} & 0 & 0 & 0 \\ -\frac{v_{xz}}{E_x} & -\frac{v_{yz}}{E_y} & \frac{1}{E_z} & 0 & 0 & 0 \\ 0 & 0 & 0 & \frac{1}{2G_{yz}} & 0 & 0 \\ 0 & 0 & 0 & 0 & \frac{1}{2G_{zx}} & 0 \\ 0 & 0 & 0 & 0 & 0 & \frac{1}{2G_{xy}} \end{bmatrix} \begin{bmatrix} \sigma_{xx} \\ \sigma_{yy} \\ \sigma_{zz} \\ \sigma_{yz} \\ \sigma_{zx} \\ \sigma_{xy} \end{bmatrix}
$$

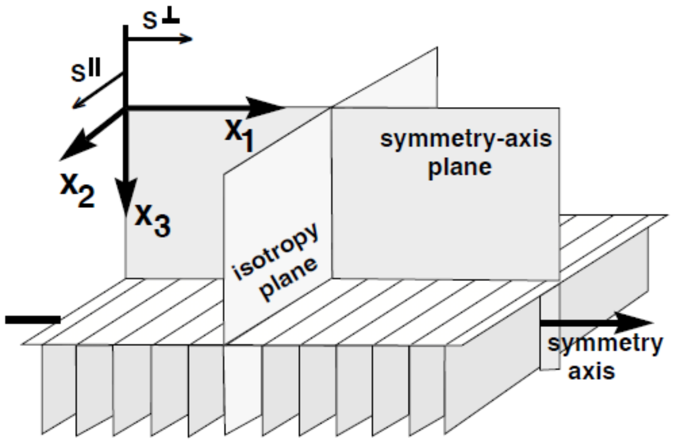

Source: Horizontal Transverse Isotropic axis defination, MIT OpenCourseWare http://ocw.mit.edu/terms/

Orthotropic constitutive equations has two orthogonal planes of symmetry and properties are independent of direction within each plane. These materials require 9 independent variables (i.e. elastic constants) in their constitutive matrices. This equation is based on orthotropic elasticity up to failure.

Thermal Material Properties

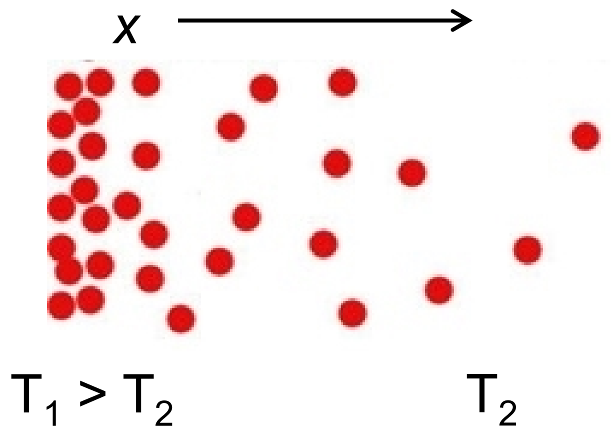

Conduction: energy transfer from a more energetic particles to less energetic particles within a material. Interactions between particles are due to a thermal gradient.

Fourier's law defines time rate of heat transfer through a material. The heat flux is proportional to the negative gradient in the temperature and to the area. The proportionality constant k is the transport property thermal conductivity W/(m °C).

$$q_x = -k\frac{dT}{dx}$$

$$\vec{q} = \mathbf{q''}$$

Heat flux **q"** is the heat transfer rate in direction *x* per unit area perpendicular to the direction of transfer. Since heat transfer rate is a vector quantity it can be written in general of the conduction rate equation:

$$\mathbf{q''} = -k\nabla T = -k\left(\boldsymbol{i}\frac{\partial T}{\partial x} + \boldsymbol{j}\frac{\partial T}{\partial y} + \boldsymbol{k}\frac{\partial T}{\partial z}\right)$$

Thermal Properties

Material	Conductivity, k W/(m °C)	Specific Heat, c_p J/(kg °C)	Density, ρ kg/(m^3)	Diffusivity, α m^2/sec 1×10^{-7}	Effusivity ε J/(m^2 °C) $\sqrt{s}$
Phenolic (resin pressed)	0.3766	1255	1380	2.174	807.667
Teflon	0.2510	1004	2170	1.152	739.6
Carbon Graphite	167.36	707.1	2250	1052	16317.6
CFRP Parallel Carbon Fibers	7	1200	1600	36.45	3666.06
CFRP Perpendicular Carbon Fibers	0.8	1200	1600	4.167	1239.45
Epoxy (hysol)	0.1945	1172	1210	1.372	525.271
Aluminum 2024 T3	121	875	2780	497.43	17156.1
Copper	397.48	384.9	8940	1155.	36982.8
Stainless Steel 304	14.644	502.1	7920	36.83	7631.1
GRP Parallel Glass Fibers	0.38	1200	1900	16.67	930.81
GRP Perpendicular Glass Fibers	0.30	1200	1900	13.16	827.04

COPV Image Registration

- Liner were digitally registered using the metal section of the scan data.
- The coordinate system was defined using:
  - A cylinder defined using points on the outer metal surface
  - A sphere (shown on right) created by averaging two spheres defined with points on the top/bottom hemispheres
  - A line defined using the tapped hole to “clock” the sample
- The origin of the coordinate system is the middle sphere center location.

Image Segmentation

- Image segmentation was performed using a combination of VGs advanced multi-material iso-segmentation, followed by region growing, and finalized with another advanced multi-material segmenting based on starting contours from region growing
- The following procedure was used:
    1. Perform advanced multi-material surface determination based on iso-values
    2. Create ROIs for the composite and liner
    3. Use region growing to remove erroneous composite definition inside the vessel
    4. Use region growing to fix any other segmentation errors
    5. Perform advanced multi-material surface determination based on starting contours (ROIs) defined above

Computed Tomography

Composite

Metal

Both

Results: COPV-4

- Pre and post pressurization XCT scans were performed
- Massive failure along weld line
- Inspection of pre-test scan for cause of failure.
- Register between scans based on natural geometric features in the composite

Pre-test

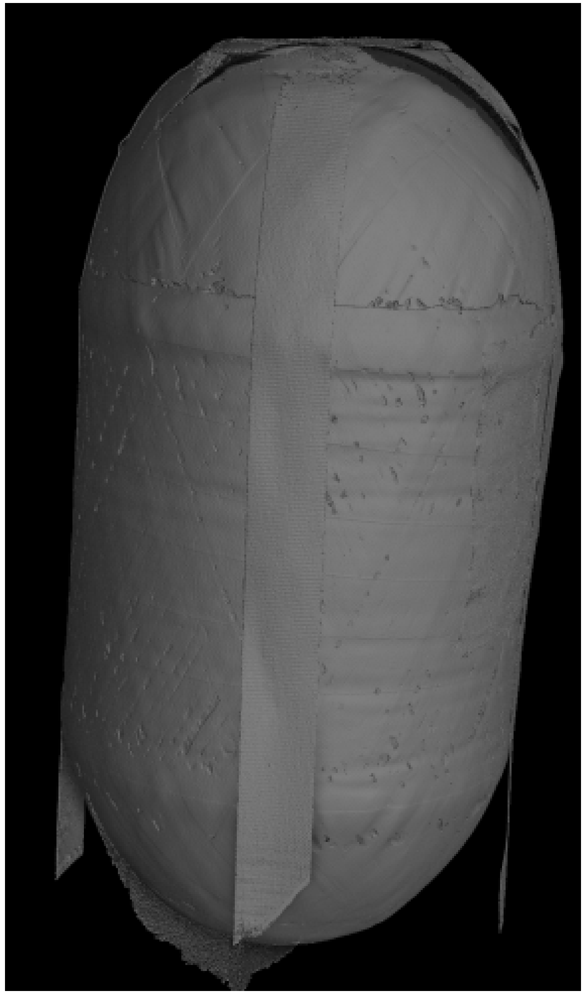

Post-test

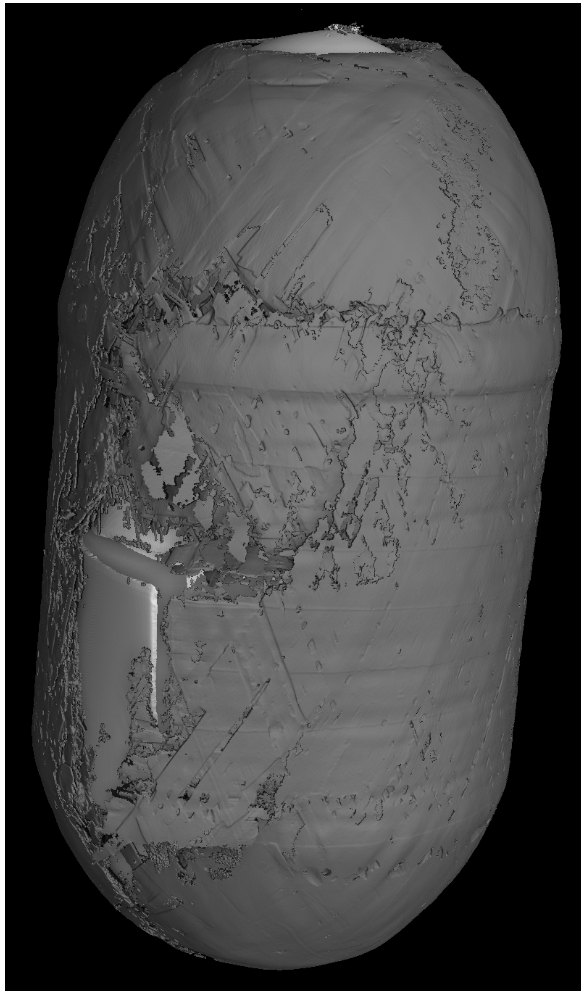

Results: COPV-4

- The weld does not fail in the region where the weld was rough (high variation in weld depth along the circumference) but instead failed in a region where the 2 liners were slightly offset
- The weld appears slightly thinner than average in the region where failure occurred
- The non-ruptured regions of the weld in the post-test scan show signs of the weld being stretched along the length of the sample and thinning
- This gives some indication of the type of failure mechanism
  - Ductile thinning of weld >> failure

Sample (COPV - 5)

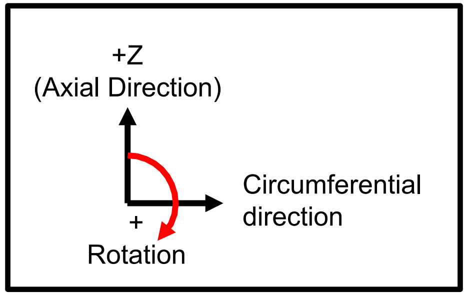

Wrap pattern on inner layers is a 20/75 degree pattern (left), whereas it moves to just a 20 degree pattern on the outer layers (right).

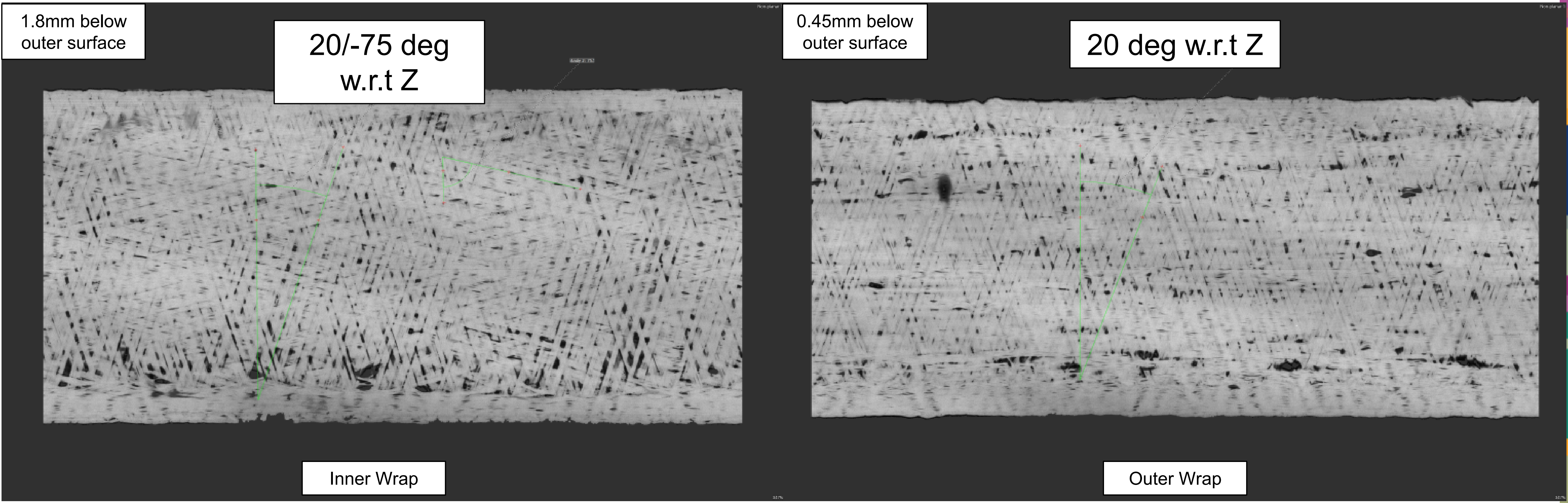

Results: COPV-5

- Low pressure failure of COPV-5 is due to break in the liner weld over significant portion of circumference
  - Curvature of the liner near the weld line suggests post test blow out

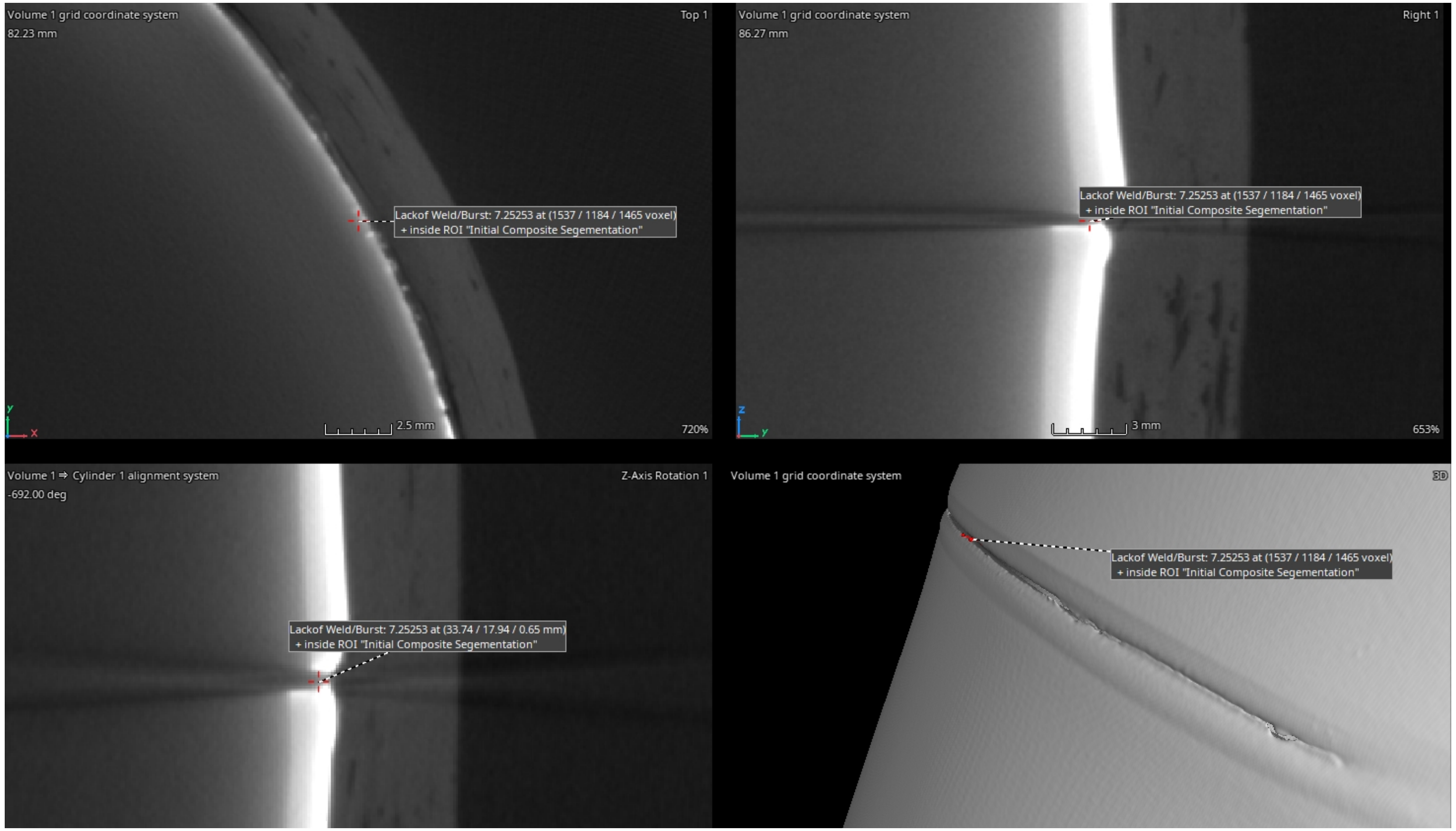

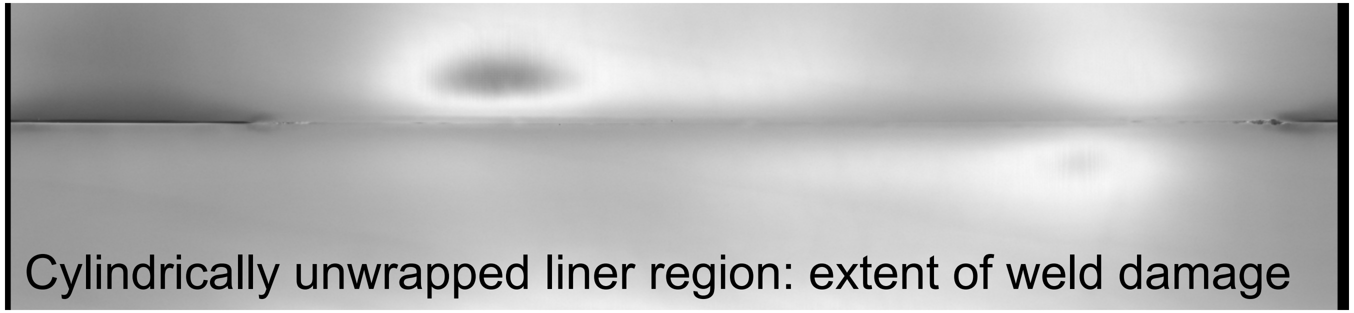
Cylindrically unwrapped liner region: extent of weld damage

Results: COPV-5

- Minor liner misalignment
- Porosity in composite wrap
  - Poorest quality near transition between cylindrical and spherical regions

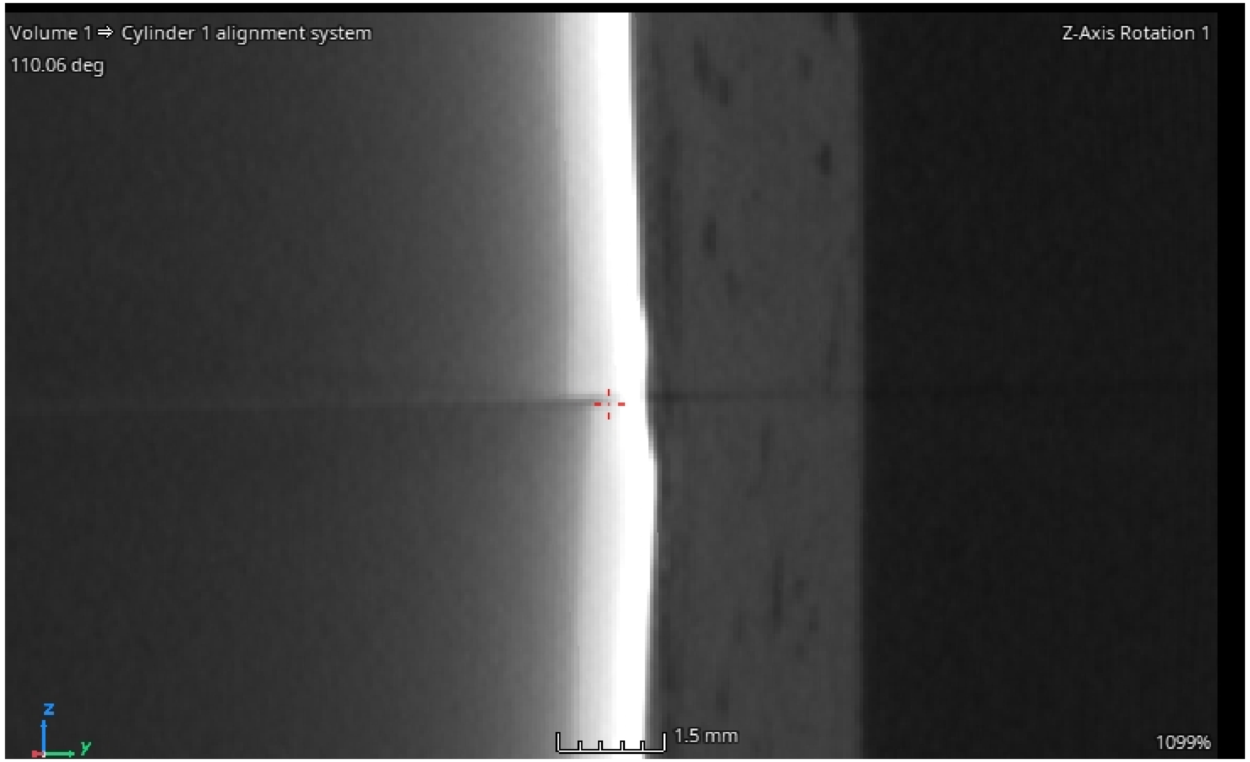

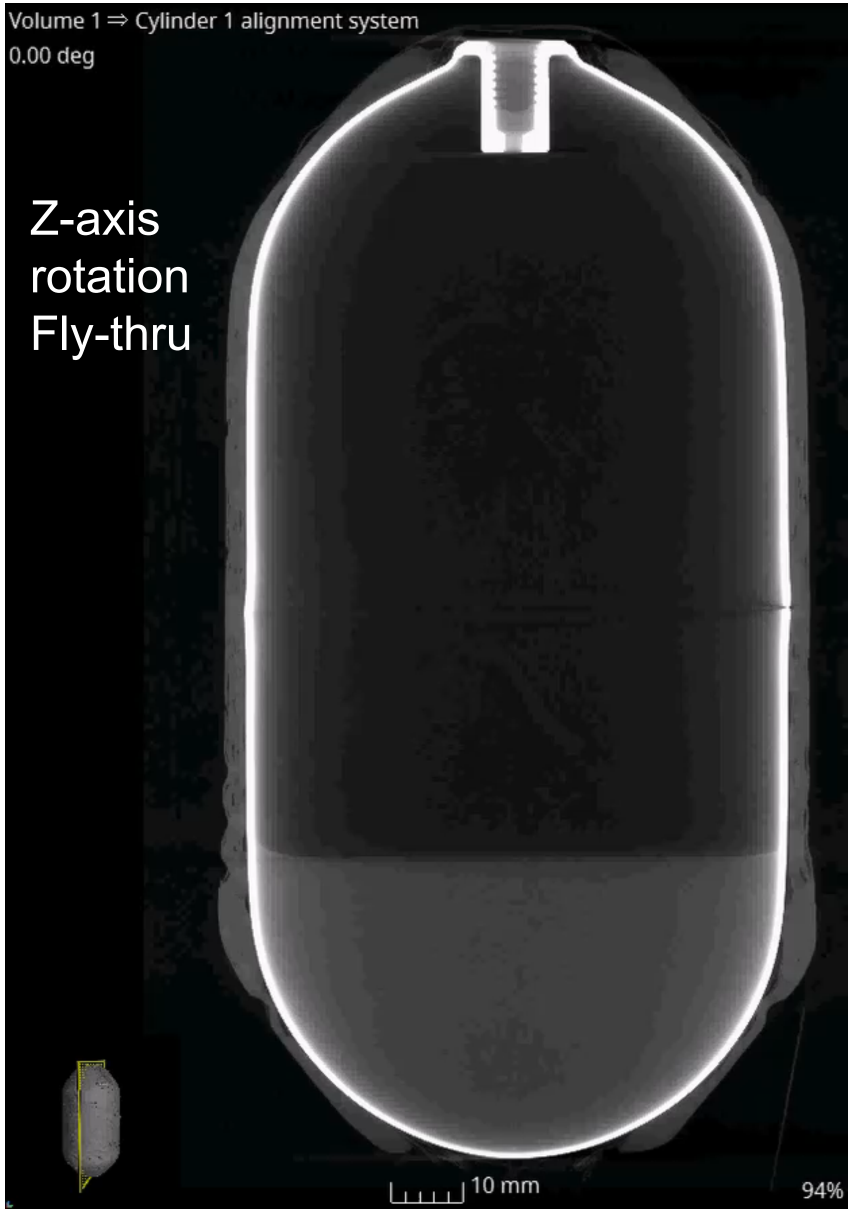

Results: COPV-5

- Broken composite near inlet end
  - No signs of liner damage in region
  - Unclear if pressure traveled "up-skin" under the composite layer from the poor weld region or if separate damage to composite
  - Could be result of poor composite bonding to liner

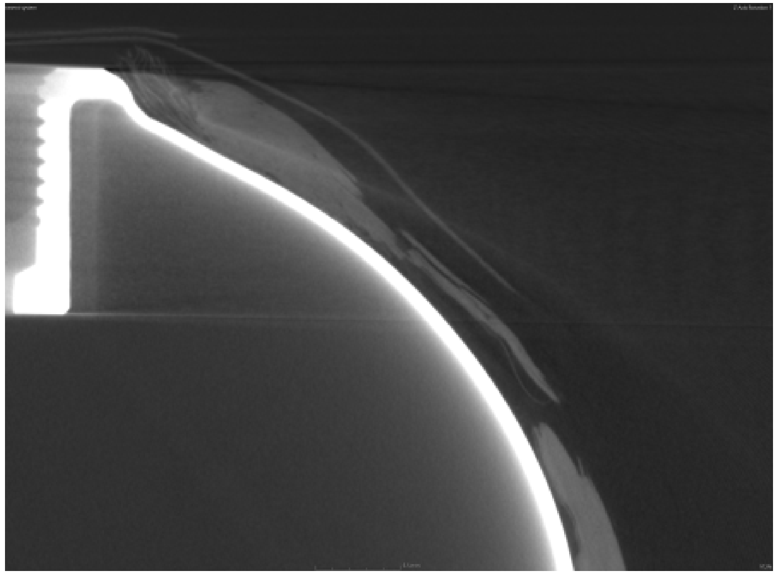

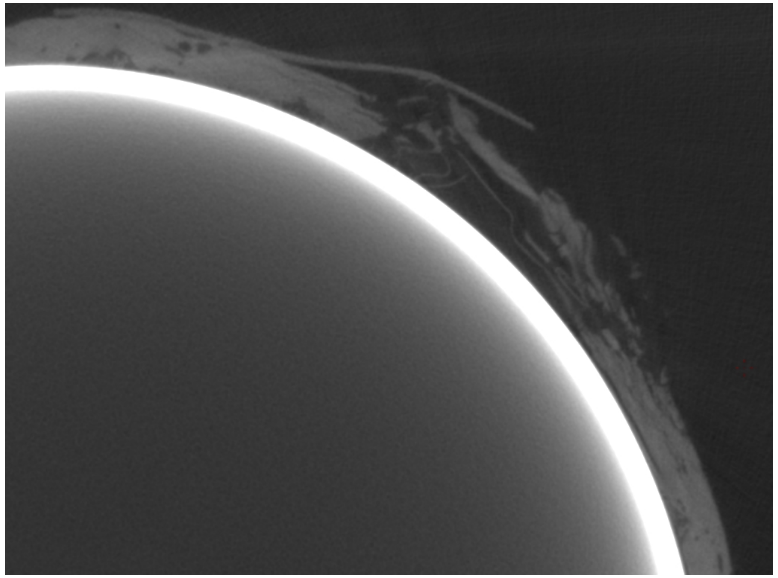

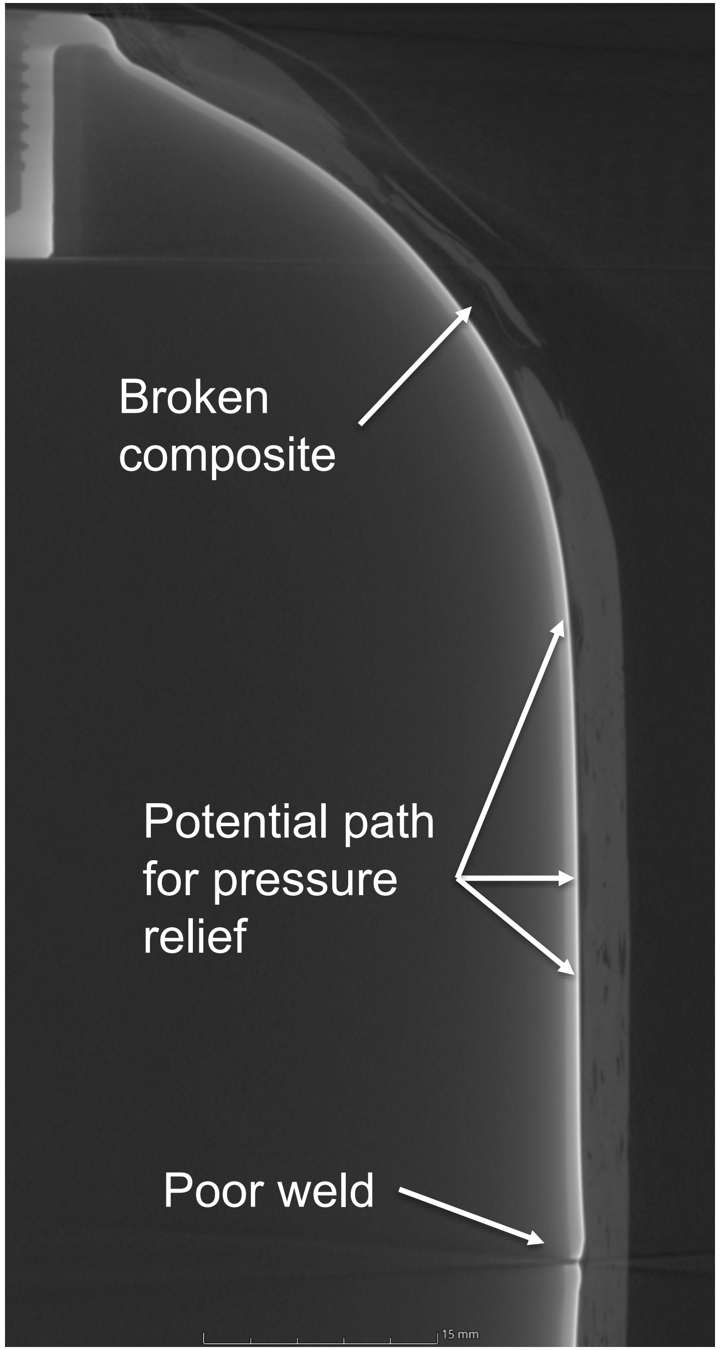

Sample (COPV - 6) with Created Defects

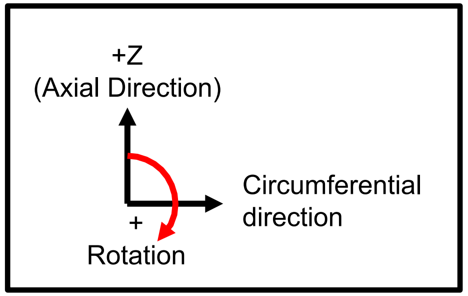

Wrap pattern on inner layers is -67 degree pattern (left), whereas it moves to a 20-75 degree pattern on the outer layers (right).

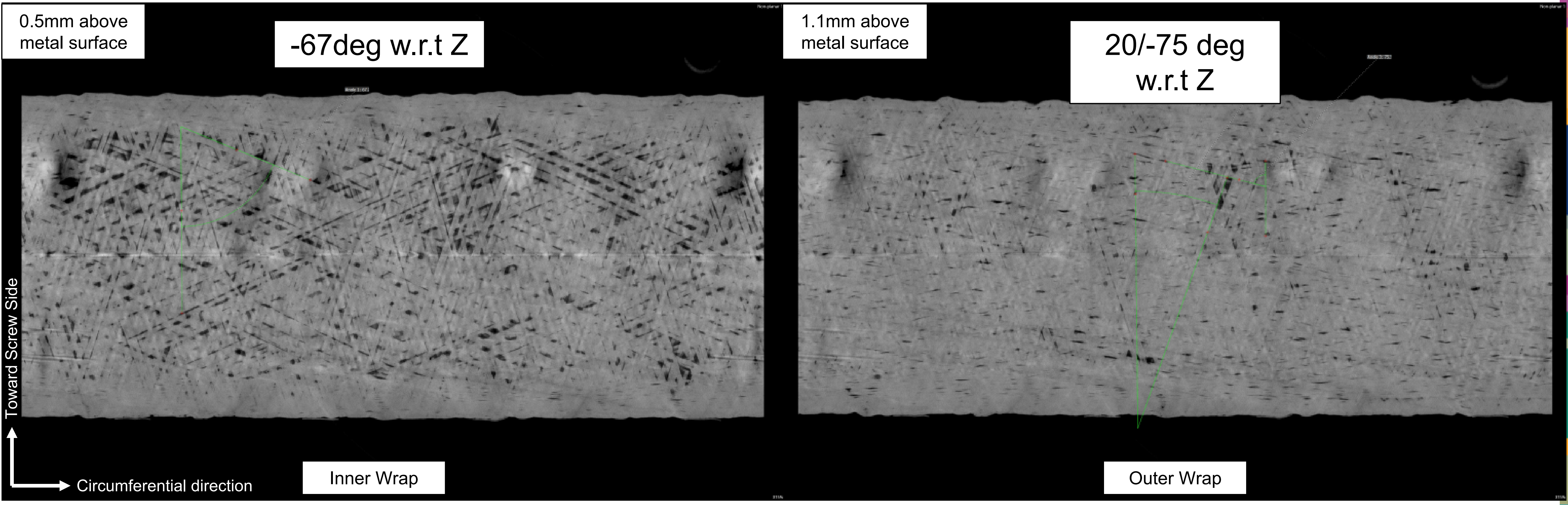

Results: COPV-6

- Some liner misalignment
- Difficult to align due to no access to internal geometry

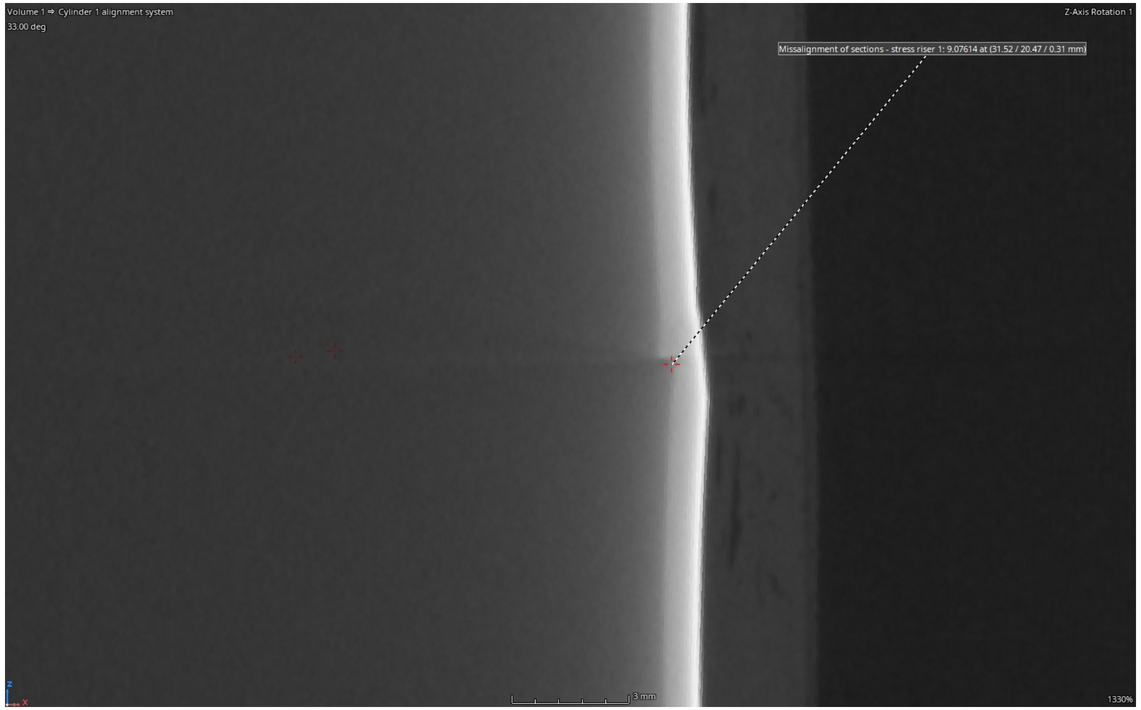

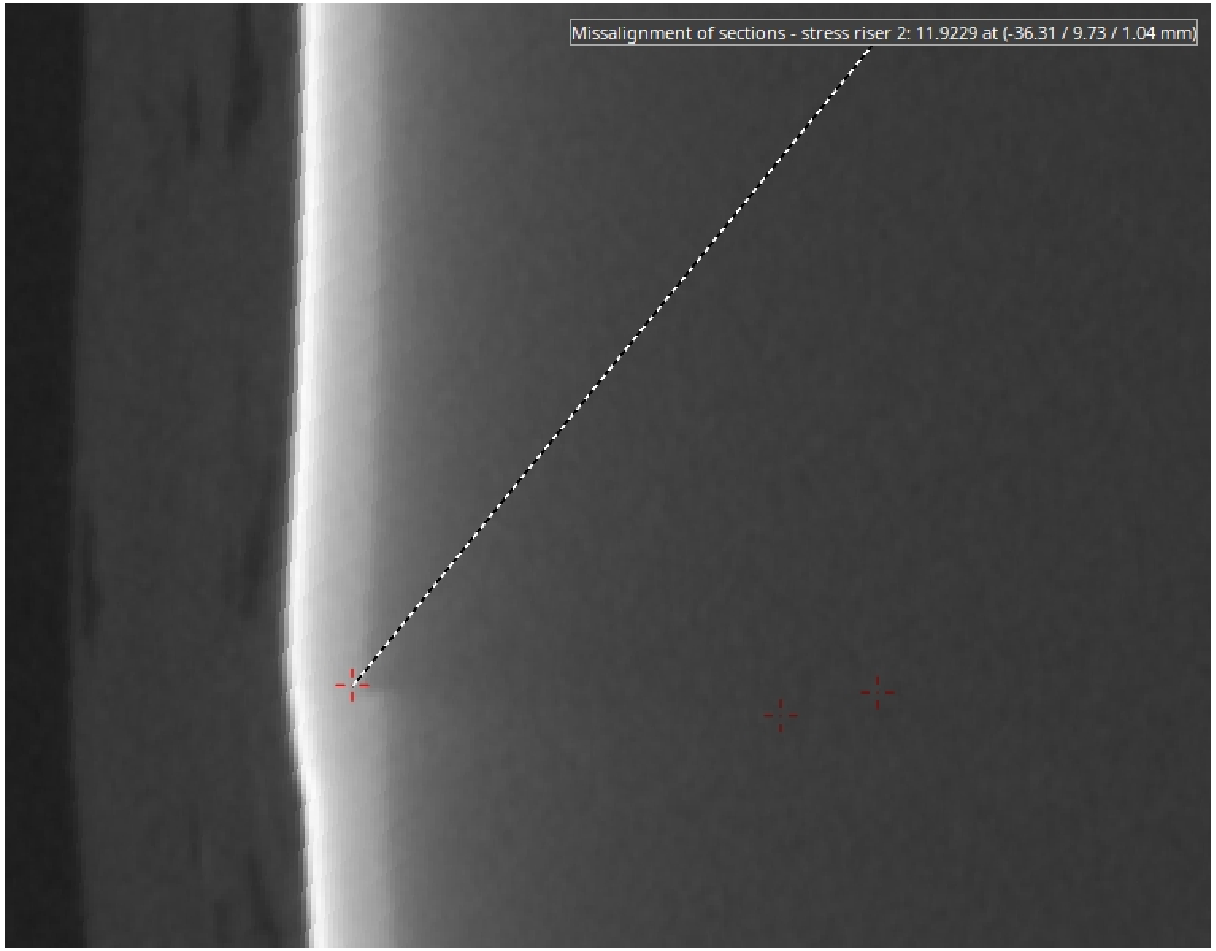

Results: COPV-6

- Poor weld penetration depth
- Possibly culprit of leaking during testing

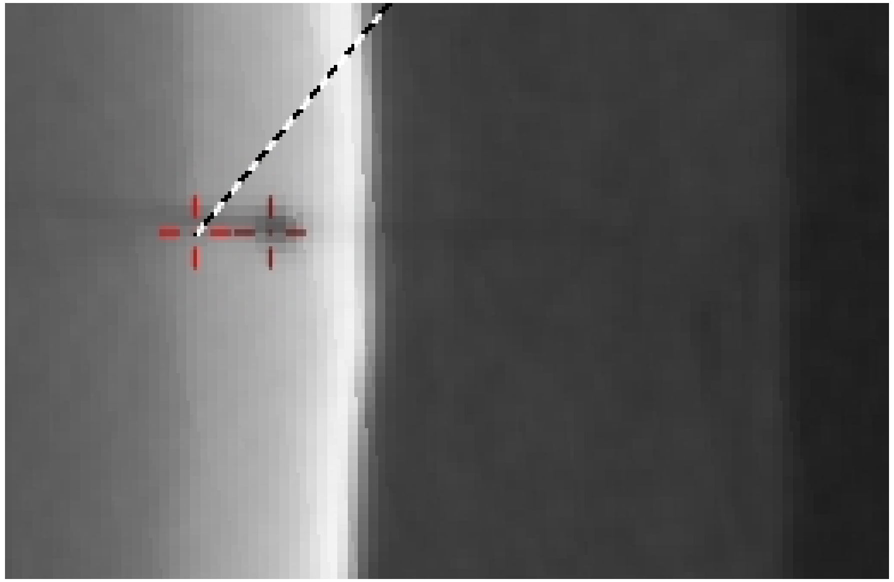

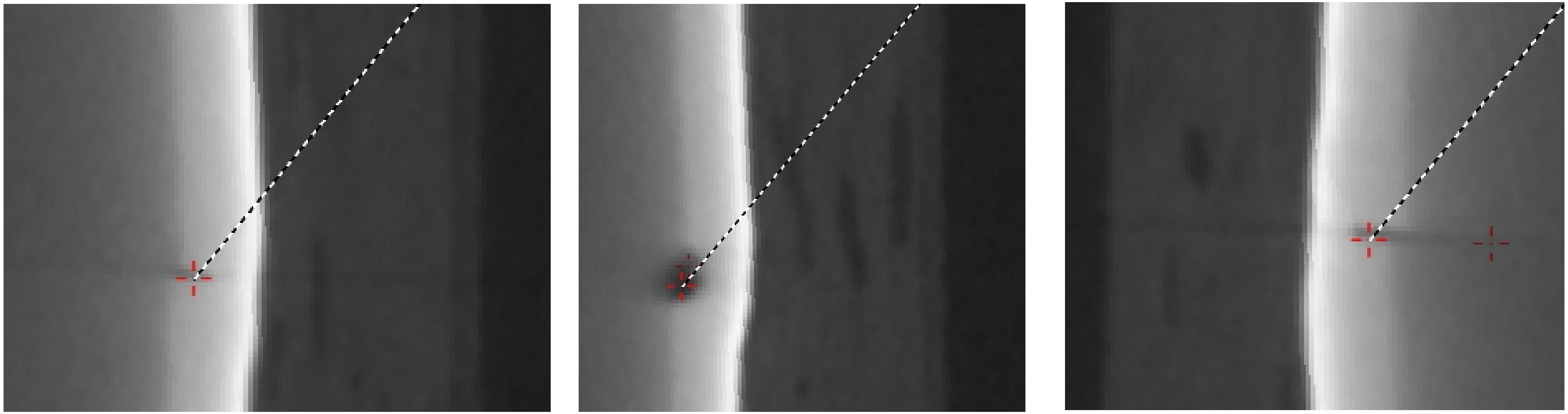

Results: COPV-6

- Some embedded porosity in the weld seam of the liner
- Composite quality poorest near transition from cylinder to sphere
  - Fly-thru videos

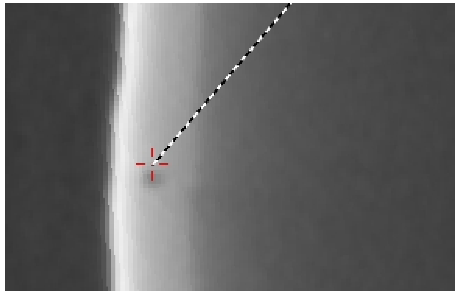
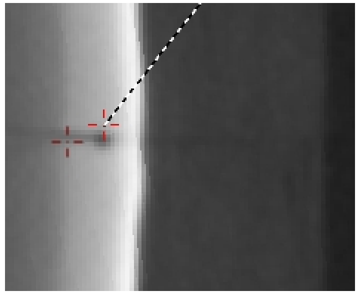

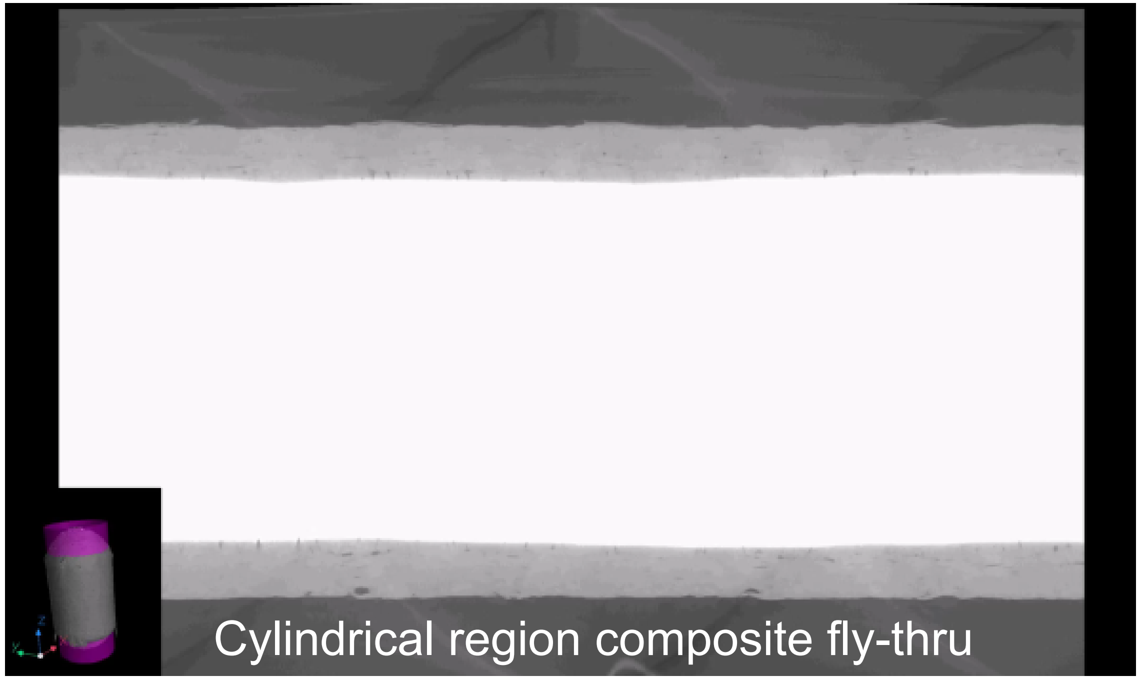

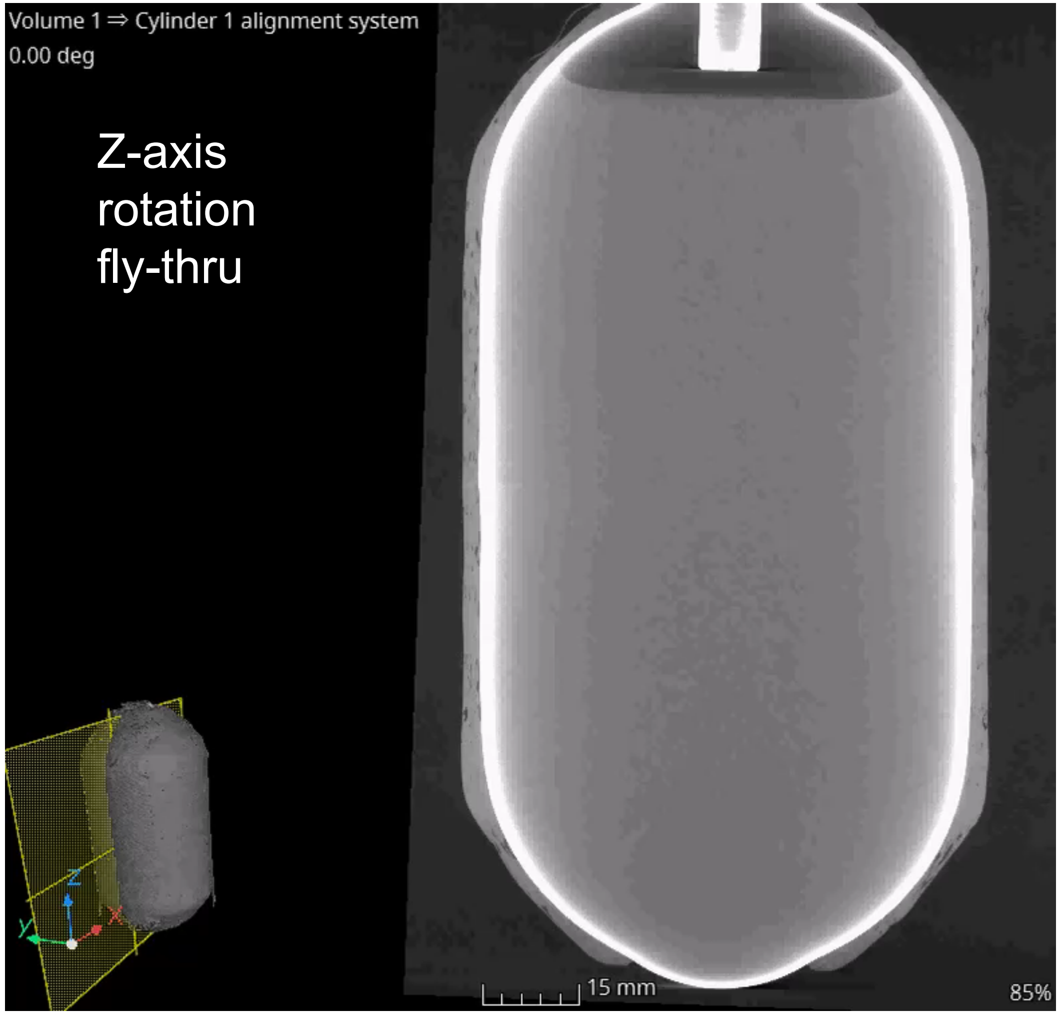

Results: COPV-6

- Composite overwrap quality degrades significantly around the transition from cylinder to sphere
  - Creates weak points for bursting if composite is not well bonded to liner
  - Potential blow out of composite

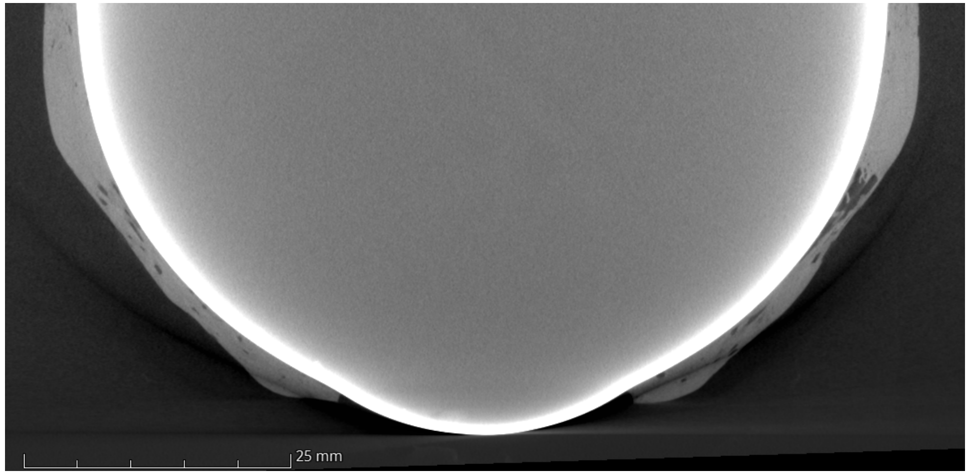

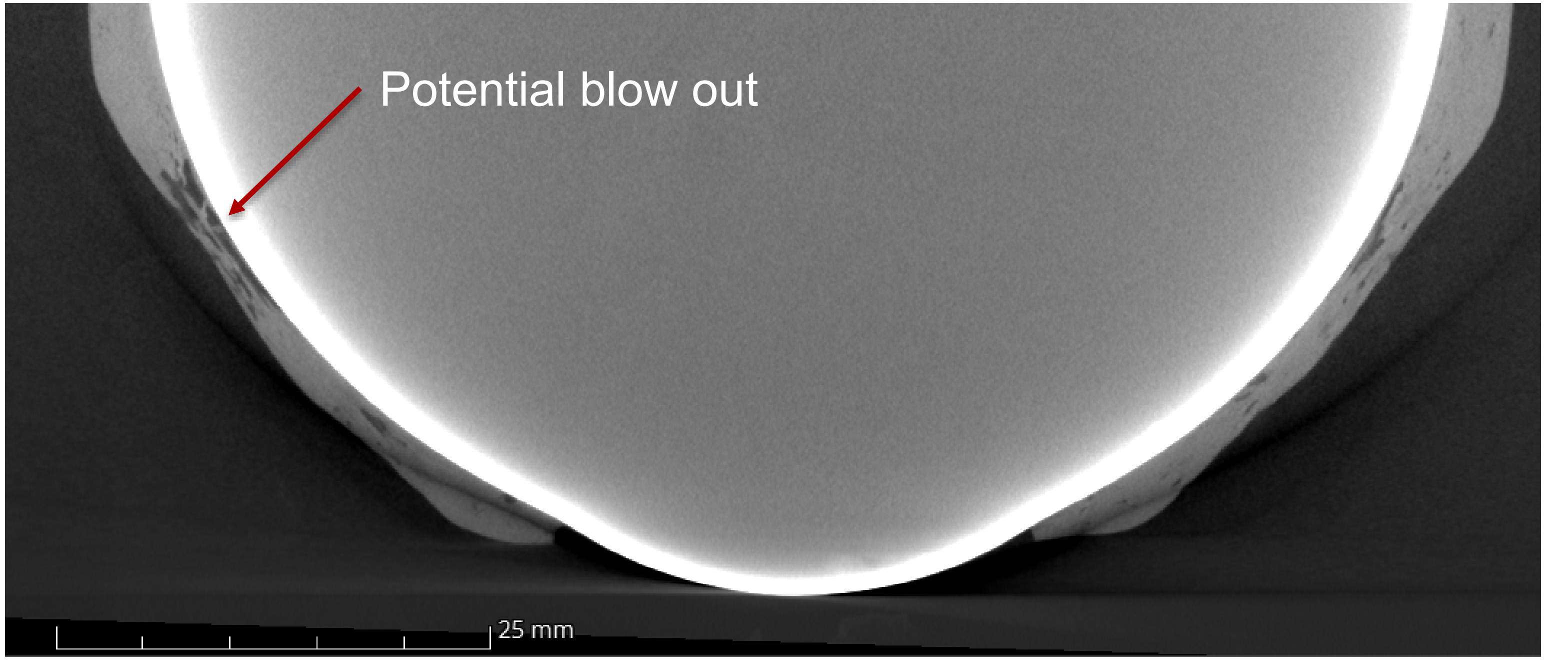

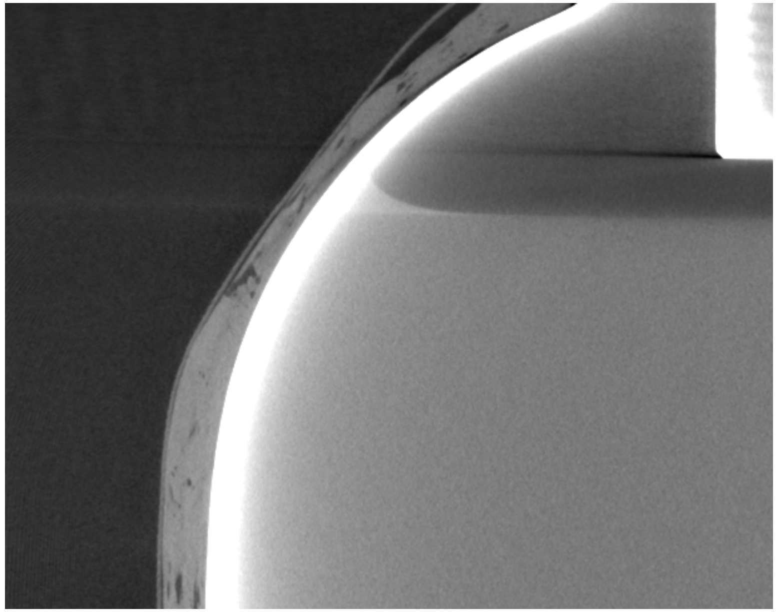

Sample (COPV - 7)

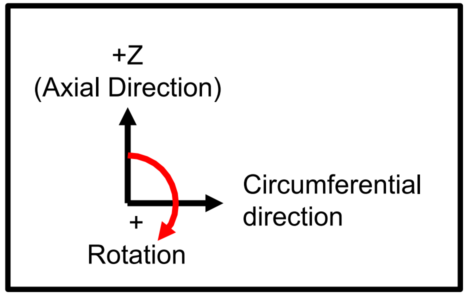

Wrap pattern on inner layers is a -25/+25 degree pattern (left), whereas it moves to just a -70/+22.5 degree pattern on the outer layers (right).

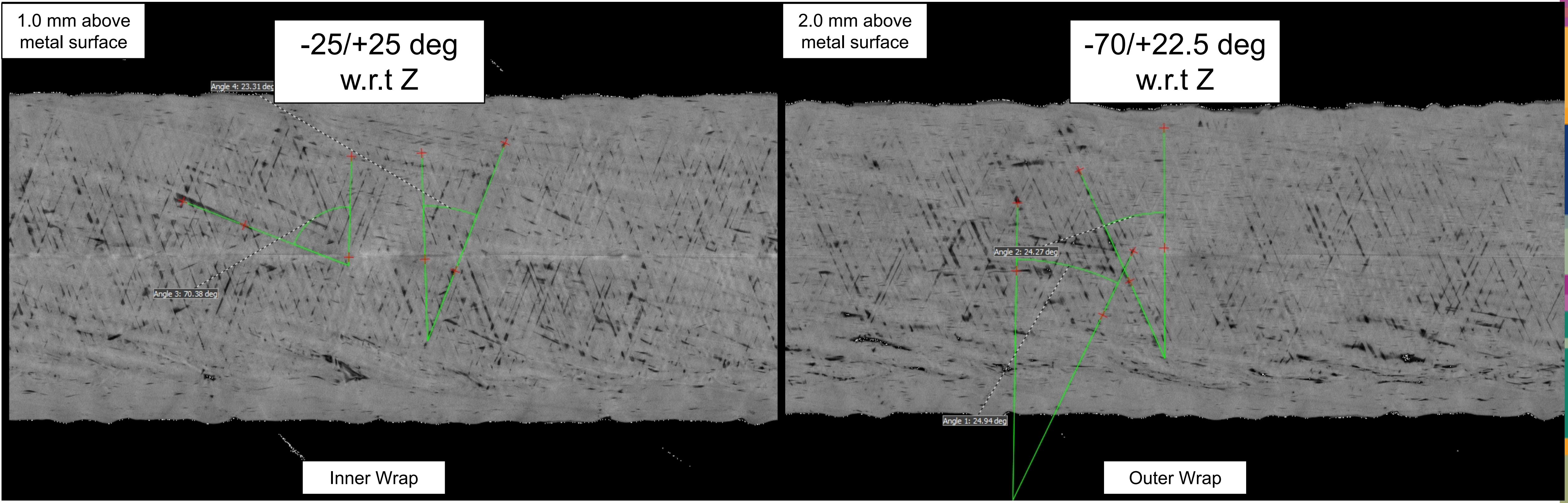

Results: COPV-7

- Vacuum debulked sample 7
- Cracking was heard from the sample while placed in the water bath for UT
- There are no signs of increased damage in the post-UT sample
- If anything the post-UT sample appears to have contracted or filled the small cracks in the pre-UT sample with water
- Appearance of small cracks may be lessened in post-UT scan due to scan quality

Results: COPV-7

- Pre-UT frequent thin cracks in composite region

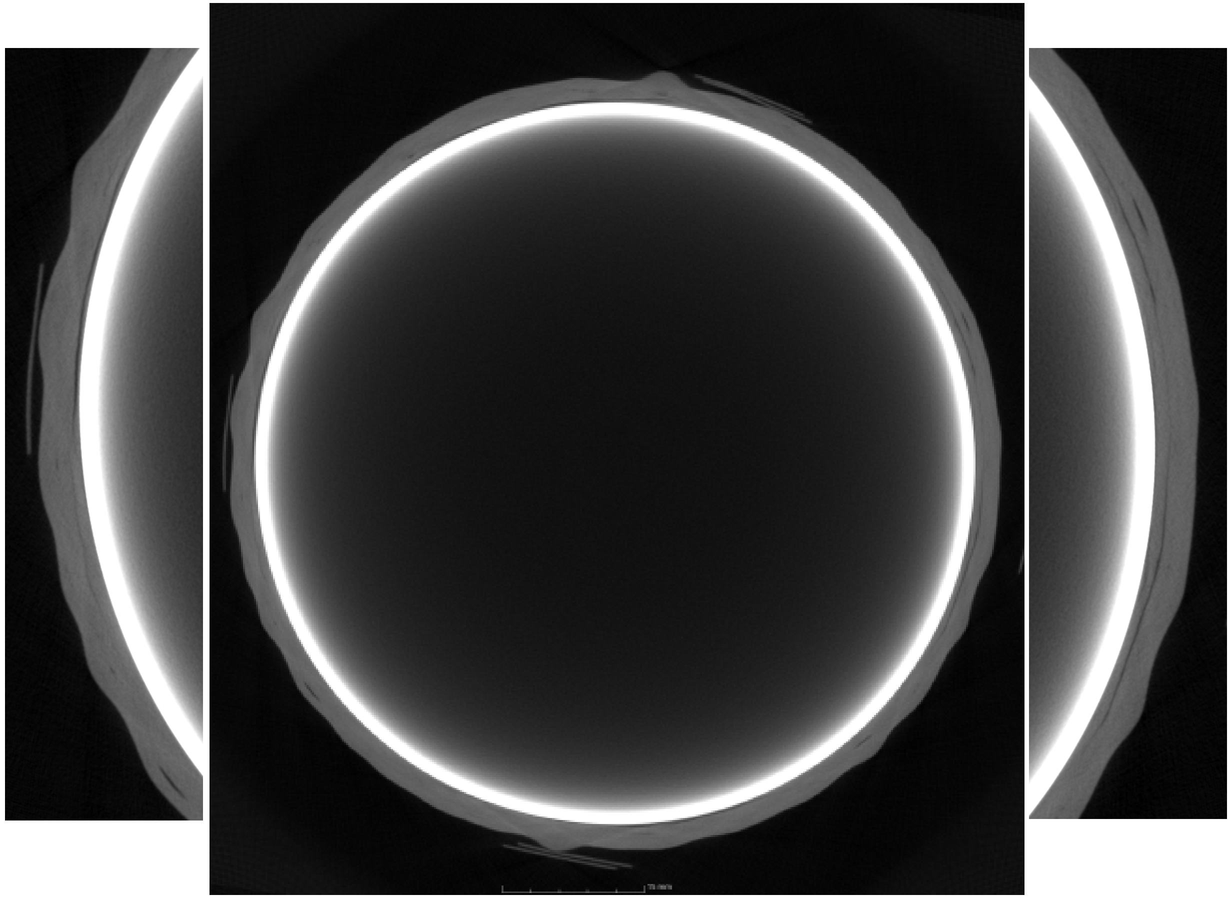

- Post-UT apparent closing of thin cracks

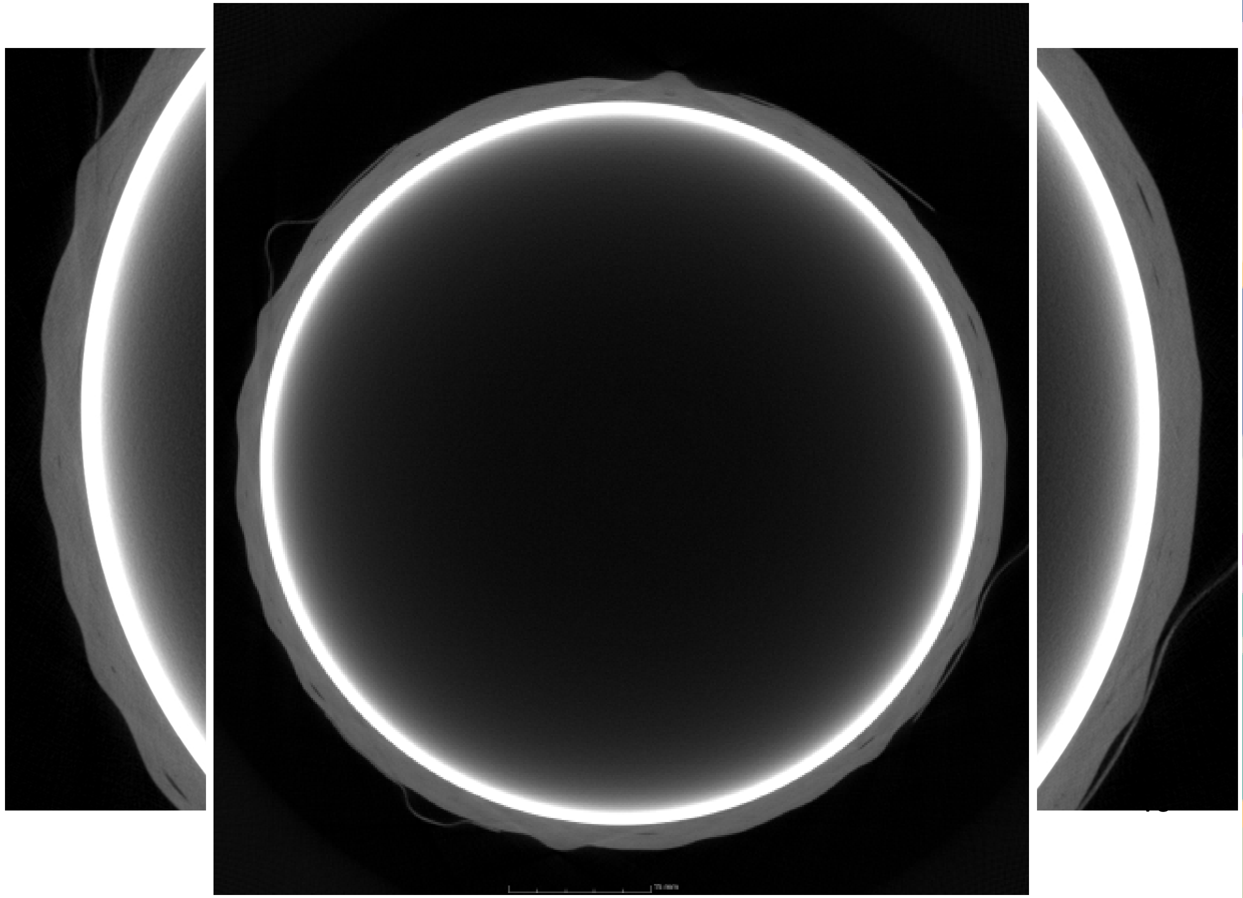

Results: COPV-7

- Pre-UT frequent thin cracks in composite region

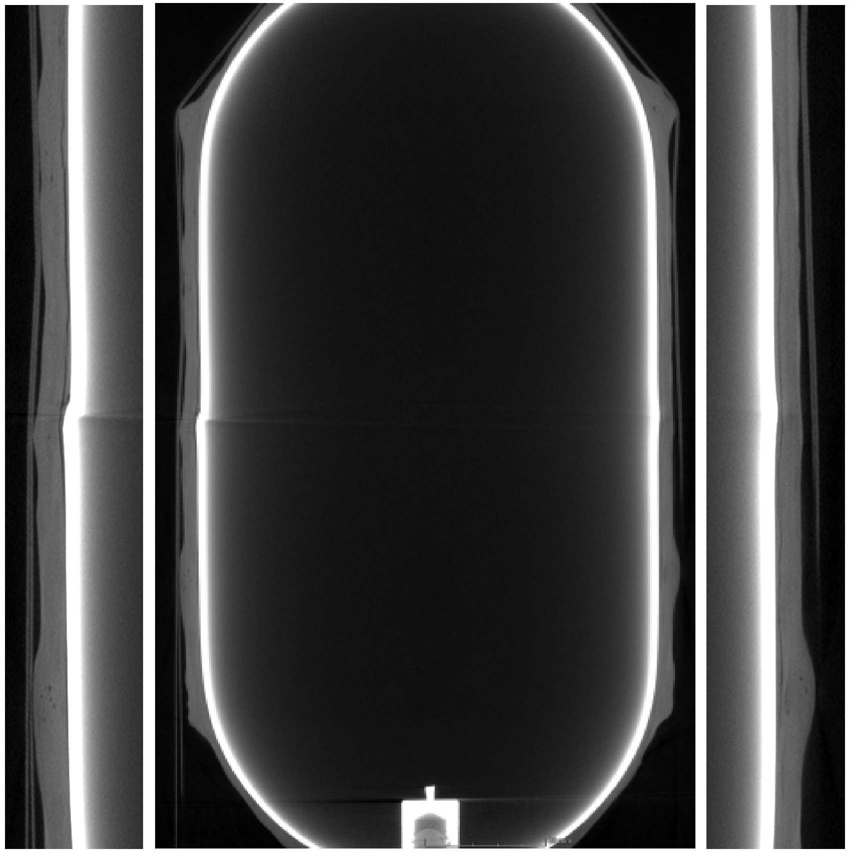

- Post-UT apparent closing of thin cracks

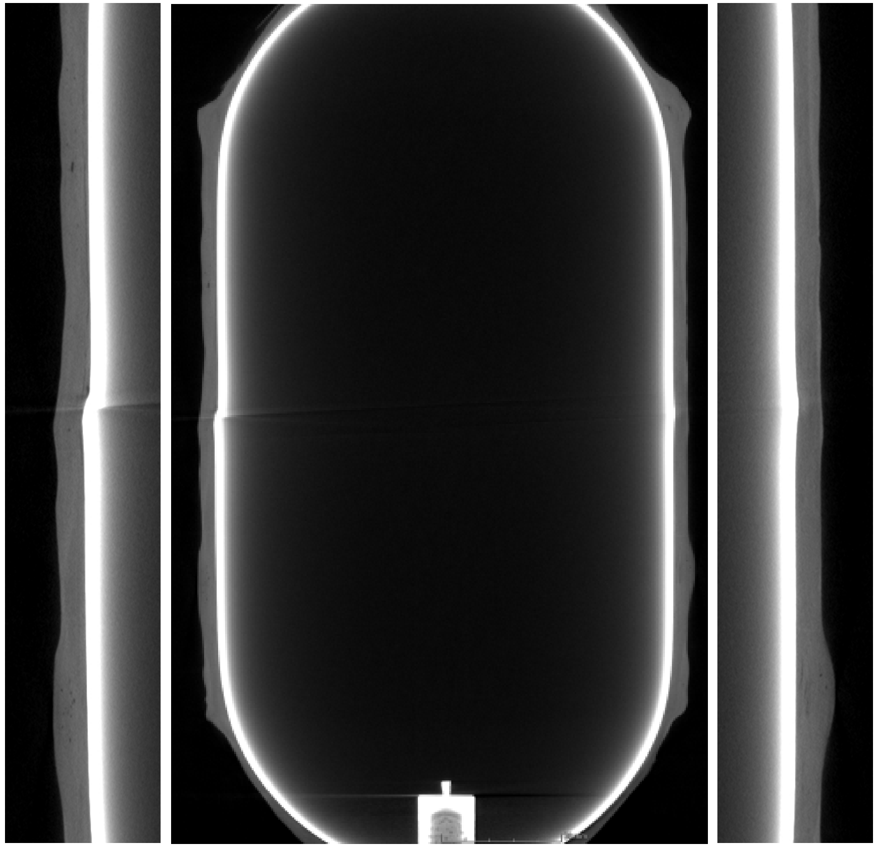

Results: COPV-7

- Think cracks between composite and liner seen in pre-UT scans
  - Not apparent in post-UT scans
  - Possible shrinkage of composite towards the liner
- Thin cracks mid composite in pre-UT scan
  - Cracks diminish in contrast in post-UT scan
  - Either a function of scan quality or partial closing of cracks
- Large cracks (pores?) unchanged

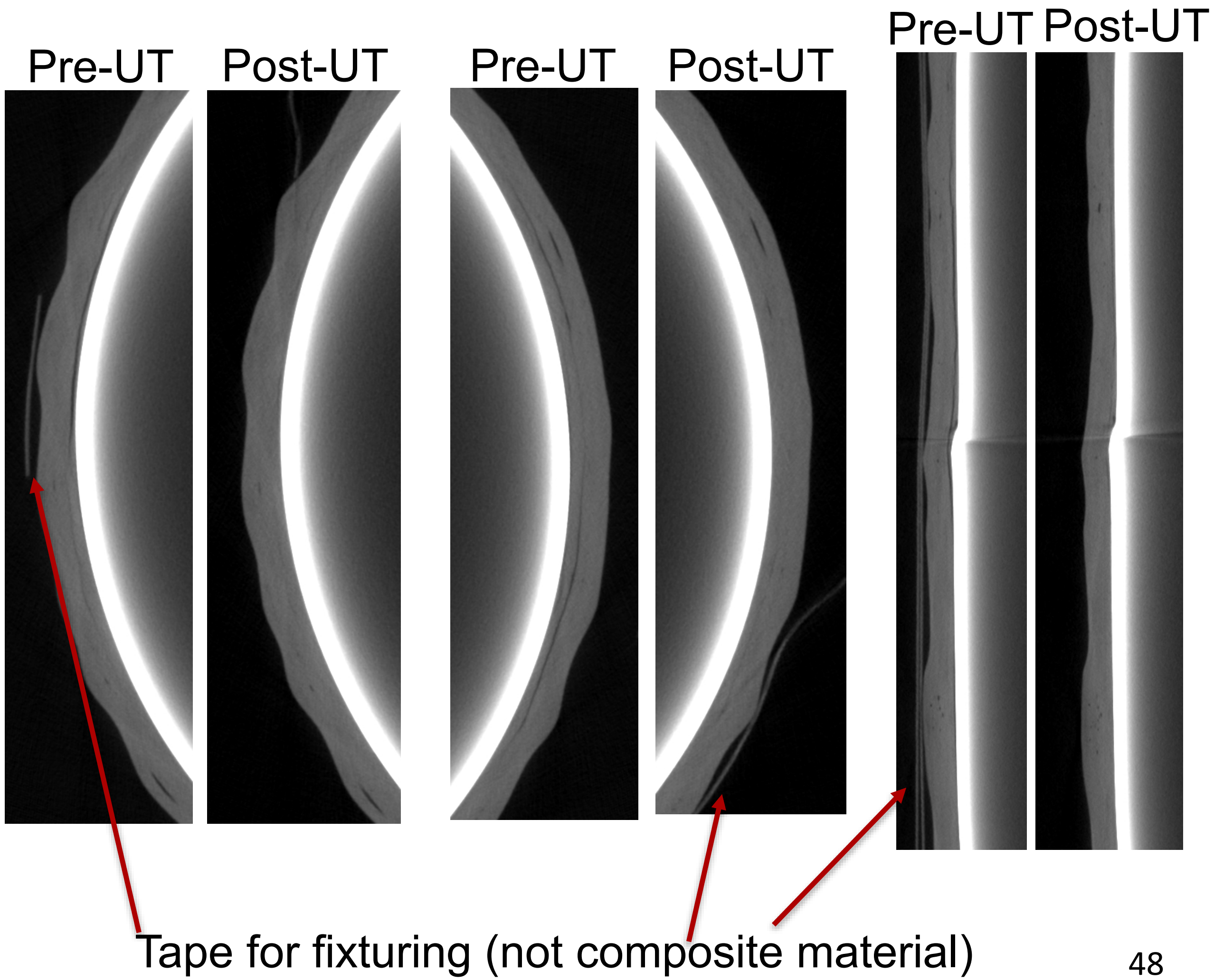

Results: COPV-7

- Pre-UT porosity seen in the liner weld

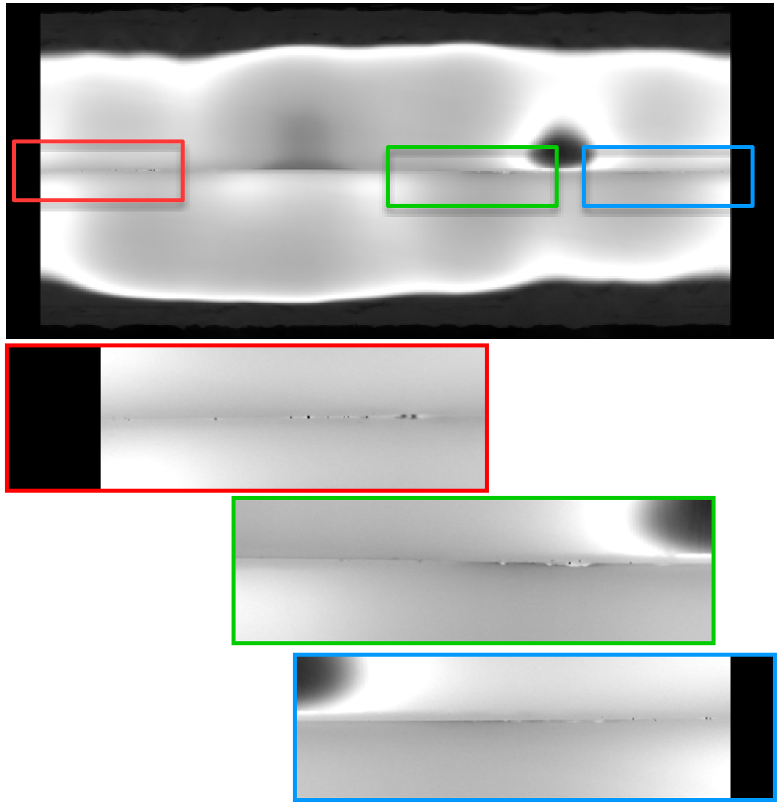

- Post-UT porosity seen in the liner weld

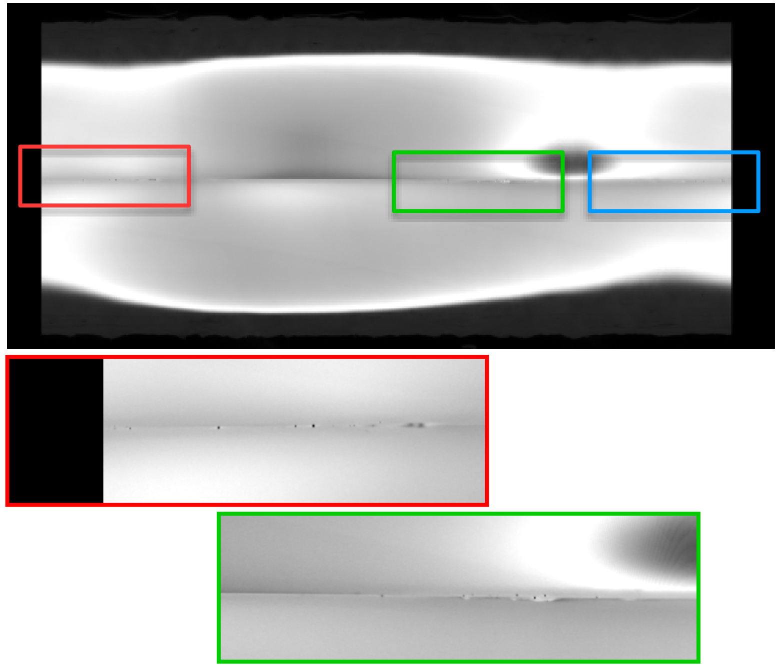

There is slightly more blur in the post-UT scan

Results: COPV-7

- Pre-UT: top view fly-thru

- Post-UT: top view fly-thru

Results: COPV-8

- Vacuum Debulked sample
- Fly-thru videos
- Poor composite quality at cylinder to sphere transition

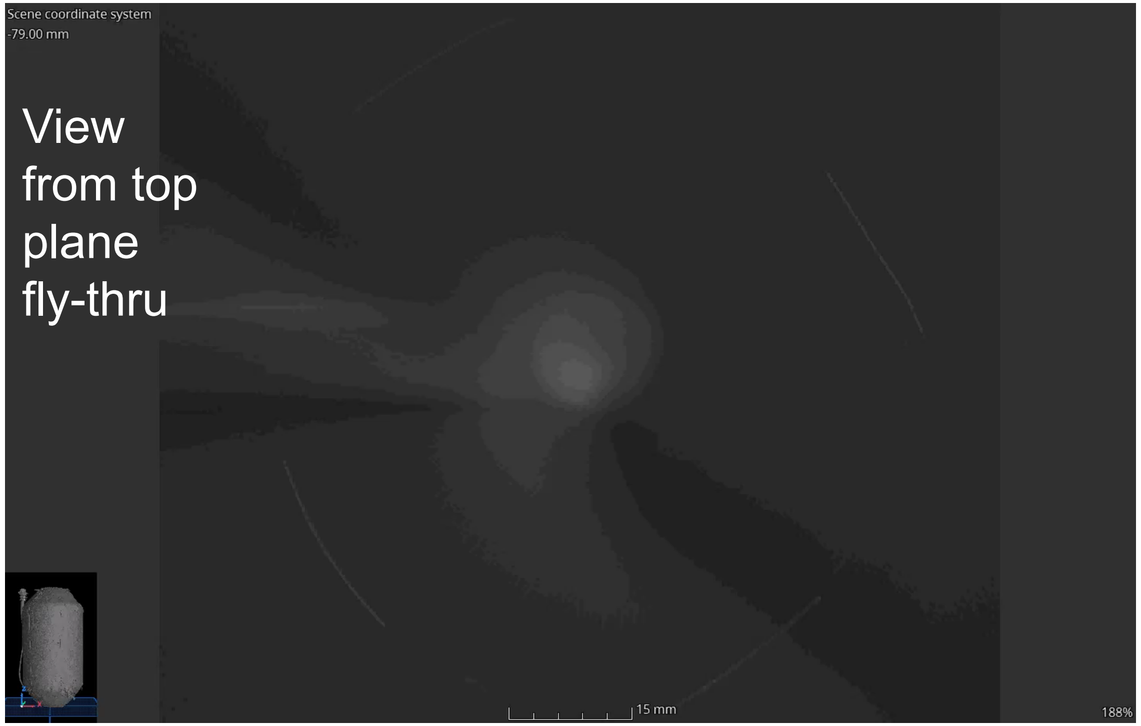

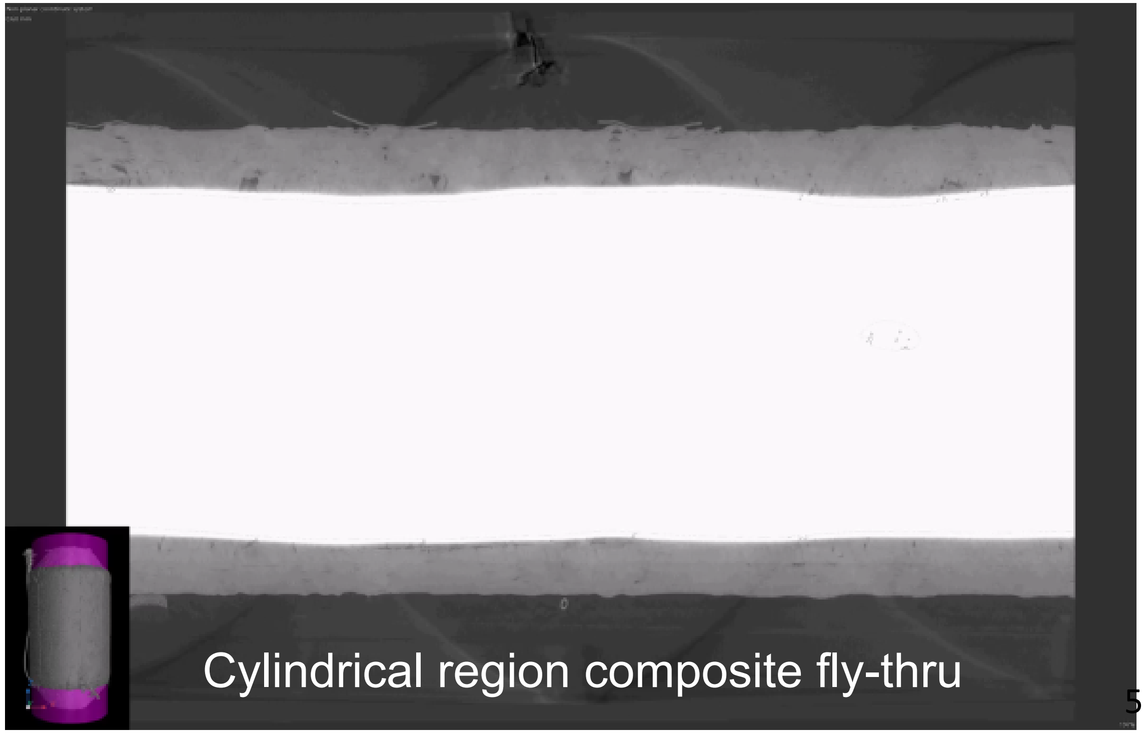

Results: COPV-8

- Composite is filled with voids/pores
- Regions of bad composite quality at transition from cylinder to sphere
- Cracking in composite near the nozzle

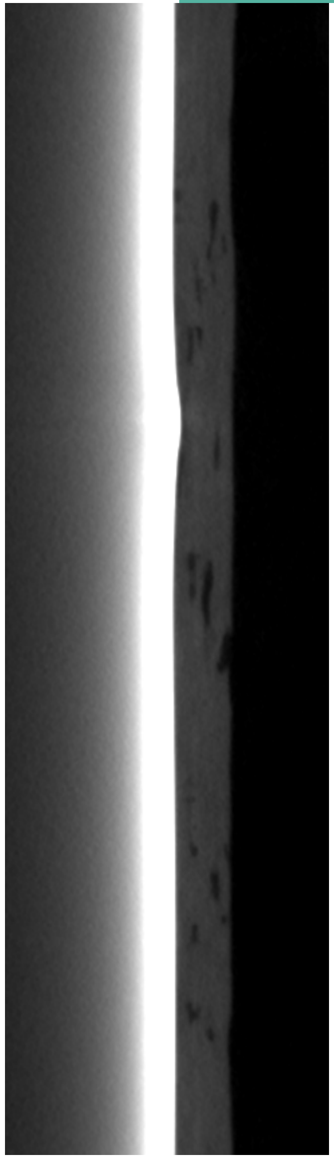

Results: COPV-8

- Weld quality concerns
- Likely locations to seed failure

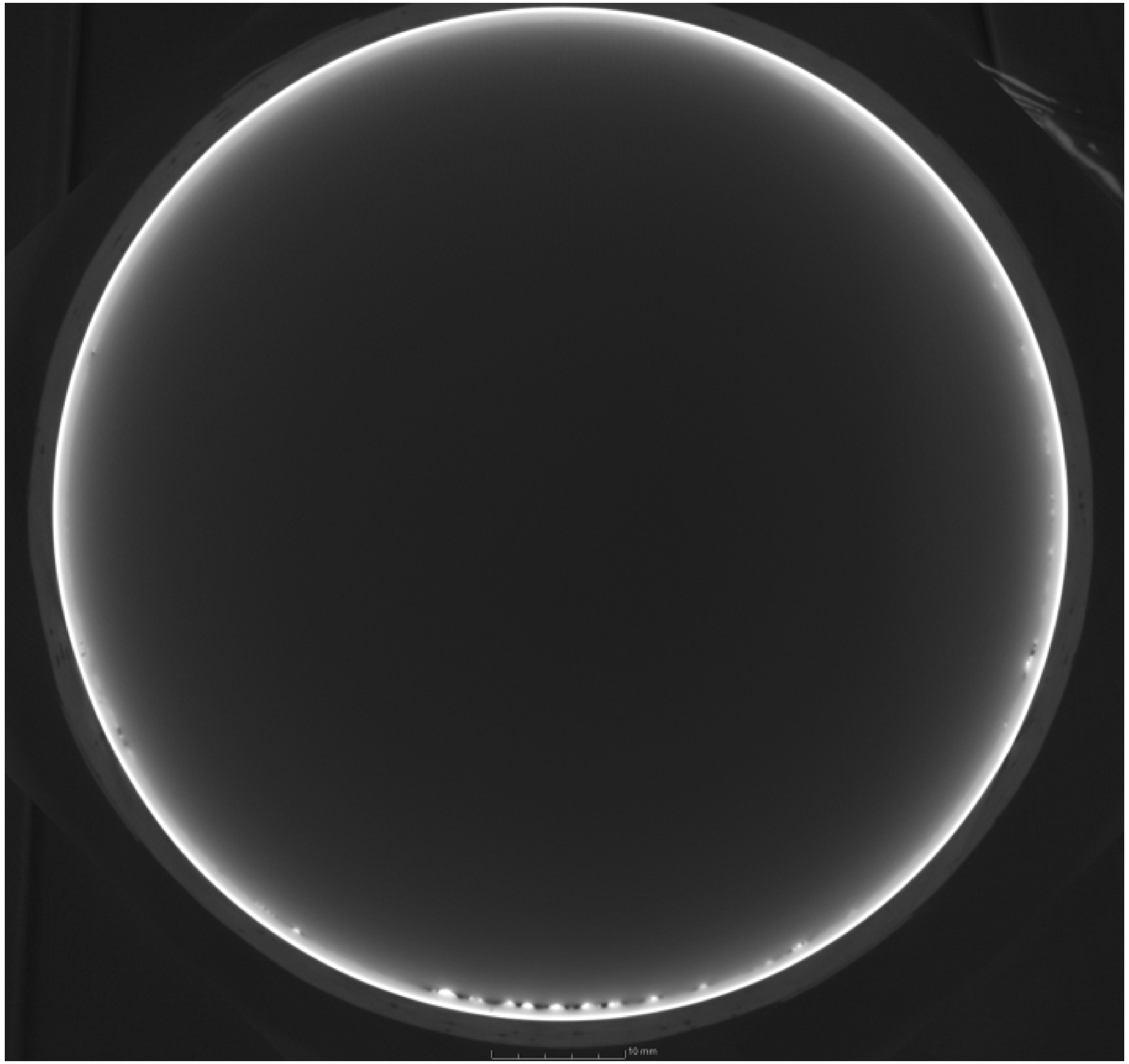

Summary: COPV-1 & COPV-5 to -8

- Over all samples there were signs of lower quality composite overlay at the transition between the cylindrical and spherical regions (biased to be on the spherical side)
- Weld quality varied across samples, but pores, liner offsets, and occasional weld spatter/roughness were common
- COPV-1 showed that the failure does not necessarily occur at the region of the rough weld
  - Other factors such as liner offset and overall weld thinness play a role
  - Weld had ductile stretching along the cylindrical axis leading weld to grow thinner
  - Thinning of the weld is likely the failure mechanism

Summary: COPV-1 & COPV-5 to -8

- COPV-5's early (low pressure) failure is a direct result of the poor weld quality
  - Pressurized water appears to have travelled along the liner of the COPV under the composite to fail at one of the poor composite quality sections at the geometric transition
  - Ability of the pressurized material to seek out weak points in the composite is a function of composite bonding to the liner
- Slow leak in COPV-6 was likely due to hole in the weld line

Summary: COPV-1 & COPV-5 to -8

- Cracking heard from COPV-7 during UT testing was likely the contraction of the composite to close the small cracks but not pores
  - Other than thermal causes is unclear why the composite would shrink
  - The cracks in the composite before the testing are likely due to the vacuum debulk process as they were not as prevalent in the other samples
- COPV-8 would likely behave similarly to COPV-7 if subjected to submerged UT testing